Origin and emplacement of igneous rocks in the central Wasatch Mountains, Utah

Thomas A. Vogel[1]*, F. William Cambray[1], and Kurt N. Constenius[2]

[1]*Department of Geological Sciences, Michigan State University, East Lansing, MI 48824, U.S.A.*

[2]*Department of Geosciences, University of Arizona, Tucson, AZ 85721, U.S.A.*

**Author to whom correspondence should be addressed: vogel@msu.edu*

ABSTRACT

The calc-alkaline igneous rocks in the central Wasatch Mountains were emplaced between 36–30 Ma. They form a belt comprised of eleven stocks and the Keetley volcanic field aligned along the crustal suture between the Archean Wyoming province and accreted Paleoproterozoic terranes. Magmatism associated with this belt and its westward continuation into the Bingham mining district has been related to mid-Cenozoic extension. These rocks consist of two types of stocks based on texture: a western type, which is coarse grained, and mostly equigranular, and an eastern type (including the Keetley volcanic rocks), which is fine grained and porphyritic. The compositional variation in the western stocks (Little Cottonwood, Alta, and Clayton Peak stocks) forms three distinct compositional groups. The compositional variation in the eastern stocks is similar to the compositional variation in the Alta stock. Major and trace element variations in these rocks resemble those of subduction-related magmas. However, the high K_2O contents and low ε_{Sr} values are not consistent with this origin. These magmas formed from melting of mafic igneous rocks. We propose that magmas were generated by decompression melting due to gravitational collapse of the crust that had been thickened during Cretaceous to early Cenozoic deformation. Magmas rose to varying levels in the crust along an east-west lineament. The igneous rocks of the central Wasatch Mountains have $\varepsilon_{Nd(t)}$ similar to most of the Phanerozoic igneous rocks in the miogeocline (MG), but have significantly lower $\varepsilon_{Sr(t)}$. That anomaly has been explained as due to melting of a basement long depleted in Rb (Farmer and DePaolo, 1983, 1984). However, the Wasatch igneous belt rocks are high-potassium, calc-alkaline rocks and all have very similar incompatible trace element patterns, whereas only a few MG rocks are calc-alkaline or high potassium. Furthermore, in the MG rocks incompatible trace element patterns are variable. One possible explanation for the dilemma of long-time depletion of Rb in these high-potassium, calc-alkaline rocks is that the crust may have been recently charged with Rb and K during the Sevier-Laramide event (100–40 Ma) by dehydration of the subducting slab. This event was followed by melting during mid-Cenozoic collapse of the orogen (ca. 40–20 Ma). The source of the magmas was melting of mafic rocks in the lower crust. Some of these magmas ponded, formed magma chambers, and differentiated. Some involved little ponding and erupted directly on the surface in the form of the Keetley volcanic field. Continued melting and extension produced new magmas from a similar crustal source. These magmas were emplaced below a series of pull-apart structures associated with strike-slip displacement along an east-west suture. This suture may have been controlled by the Archean-Proterozoic boundary. Some magma bodies were emplaced quickly to the surface without significant fractionation. Others coalesced and fractionated over a protracted period of time. These magma bodies interacted with crustal rocks, and differentiated to relatively evolved compositions.

KEY WORDS: Calc-alkaline magmas, magma evolution, magma generation, magma emplacement, magma ascent, crustal melts, pull-apart structures, extensional duplexes, strike-slip faults, Wasatch Mountains, Sevier orogenic belt.

INTRODUCTION

In the central Wasatch Mountains a series of eleven stocks (Figs. 1 and 2) and the Keetley volcanic field (along with abundant dikes and other minor intrusions) are exposed along an east-west belt extending westward from the Uinta arch. This belt is coincident with the Uinta-Cortez axis of Roberts et al. (1965) which, according to Presnell (1998), marks the boundary between the Archean Wyoming province to the north and Paleoproterozoic Yavapai province to the south. The cratonic margin extends westward into central Nevada and eastward into northeast Utah where it is coincident with the Uinta aulacogen (Presnell, 1998). The Uinta-Cortez axis has been periodically active from Paleoproterozoic through Cenozoic time (Roberts et al., 1965; Wright and Snoke, 1993; Stone, 1993; Presnell, 1998), and the igneous intrusions and extrusions of the central Wasatch Mountains are the most recent evidence of this activity.

The igneous rocks of the central Wasatch Mountains are calc-alkaline, high-potassium rocks (Figs. 3 and 4). They formed between 36–30 Ma. Subsequently, middle to late Cenozoic flexural-isostatic uplift associated with the Wasatch normal fault produced a regional tilt to the east (Parry and Bruhn, 1987; John, 1989a). The Little Cottonwood stock at the western end of this belt is the most deeply exposed, having been emplaced at a depth of about 11–5.6 km (Parry and Bruhn, 1987; John, 1989a). To the east, the other magma bodies of this belt are exposed at shallower levels, the easternmost consisting of the extrusive Keetley volcanic field. Igneous intrusions in the central Wasatch Mountains are oriented in an east–west-trending belt.

The late Cretaceous to middle Cenozoic magmatism and deformation in the Cordillera of the southwestern United States and Mexico have been attributed to initial subduction of a low-angle slab and its subsequent rollback. The low-angle subduction is associated with contraction, and rollback with extension (Coney and Reynolds, 1977; Engebretson et al., 1985; Dickinson, 1991; Wernicke, 1992; Sterne and Constenius, 1997). Constenius (1996, 1998) proposed a similar sequence of contraction and extension for the central Wasatch Mountains: contraction related to subduction, followed by extension related to gravitational collapse of the Cordilleran fold-and-thrust belt. To explain the southward migration of igneous belts in the Great Basin, several workers (e.g., Cross and Pilger, 1978; Lipman, 1980, 1992; Best and Christiansen, 1991) suggested that this migration was related to the steepening and foundering of the Farallon plate beneath North America. Rowley (1998) reviewed these igneous belts and suggested that they are closely associated in space and time with linear zones of structural discontinuities produced by crustal extension.

Presnell (1998) reviewed the evidence that the magmatism represented by the igneous rocks of the central Wasatch Mountains and their counterparts westward into the Bingham district is related to Cenozoic northwest-southeast extension. The evidence includes: the majority of the ore-bearing veins and lodes associated with the Bingham district strike northeast, and veins and dikes associated with the igneous rocks of the central Wasatch Mountains, which both pre- and post-date emplacement of the stocks, also strike northeast. Studies of the Bingham District conclude that the porphyry copper deposit was emplaced during a period of northwest-southeast extension (Presnell, 1992) and associated alkalic volcanism was the product of rifting (Waite et al., 1998). Based on examination of structural and stratigraphic data and the stratigraphic record preserved in half grabens, Constenius (1996, 1998) identified a separate west-southwest–east-northeast extension that began in the late Eocene (ca. 40–38 Ma) and continued through the middle Miocene (ca. 20 Ma).

In this paper we suggest that the magmas of the central Wasatch Mountains were generated by decompression due to mid-Cenozoic gravitational collapse of the crust that had been deformed and thickened during the Sevier orogeny. These magmas were emplaced in a series of collapsed extensional duplexes associated with strike-slip motion along an east-west suture, which marks the boundary between Paleoproterozoic and Archean crust. During the processes of ascent, storage, and emplacement, magmatic differentiation gave many of the stocks their distinctive chemical composition with respect to major elements, although the magmas retained a trace element chemical signature indicative of their common origin. This paper focuses on the igneous rocks of the central Wasatch

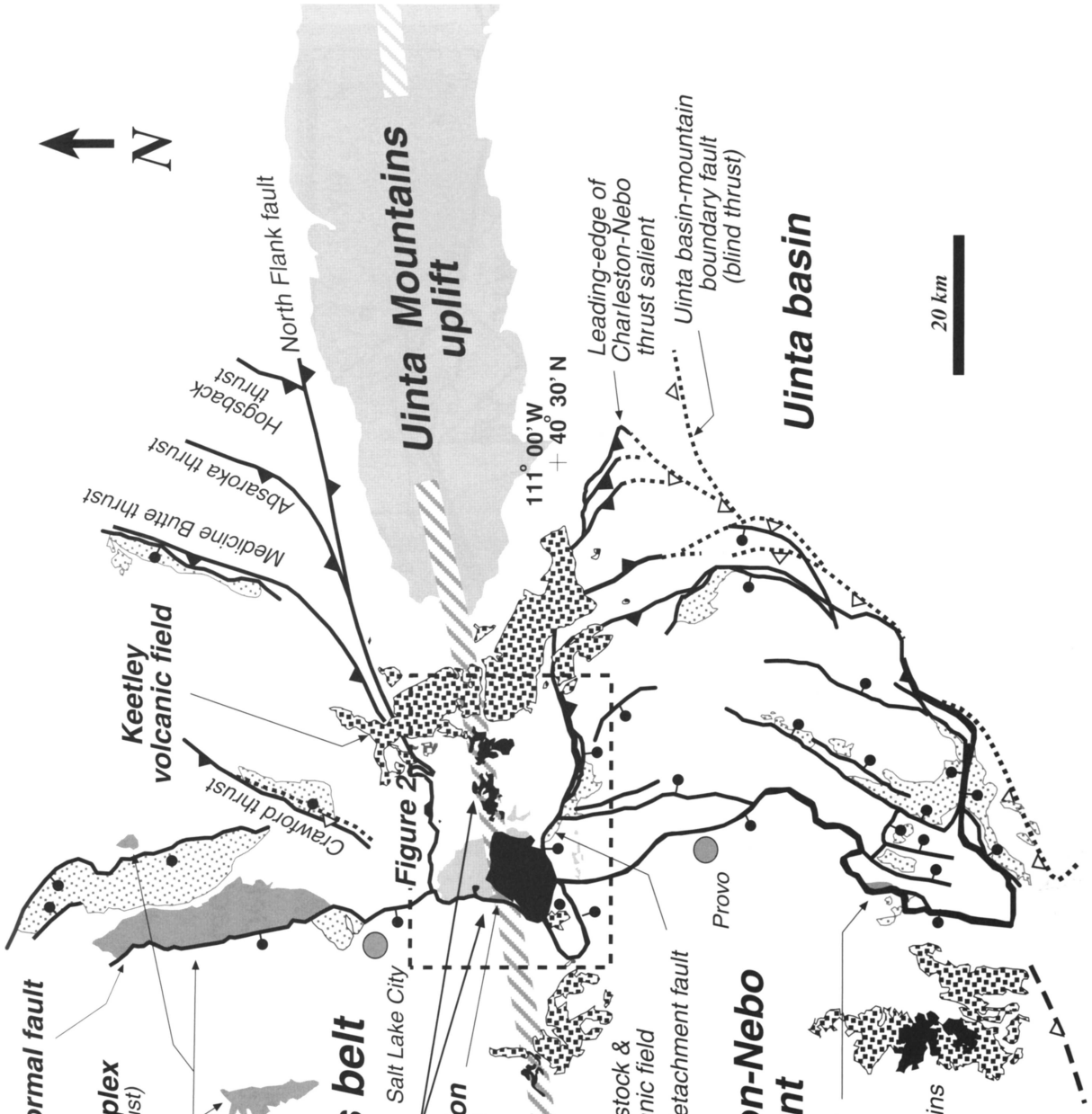

Figure 1. Geologic index map of major tectonic elements in north-central Utah. Key to units: Precambrian crystalline rocks, medium gray; Precambrian sedimentary rocks, light gray; Eocene-Oligocene intrusive igneous rocks, black; Eocene-Oligocene extrusive igneous rocks, heavy square stipple; Eocene-Oligocene volcaniclastic rocks and extensional basin fill deposits, light check stipple. Inferred position of the Uinta-Cortez axis shown as a candy-cane line. Map adapted from Hintze (1988) and Constenius (1998).

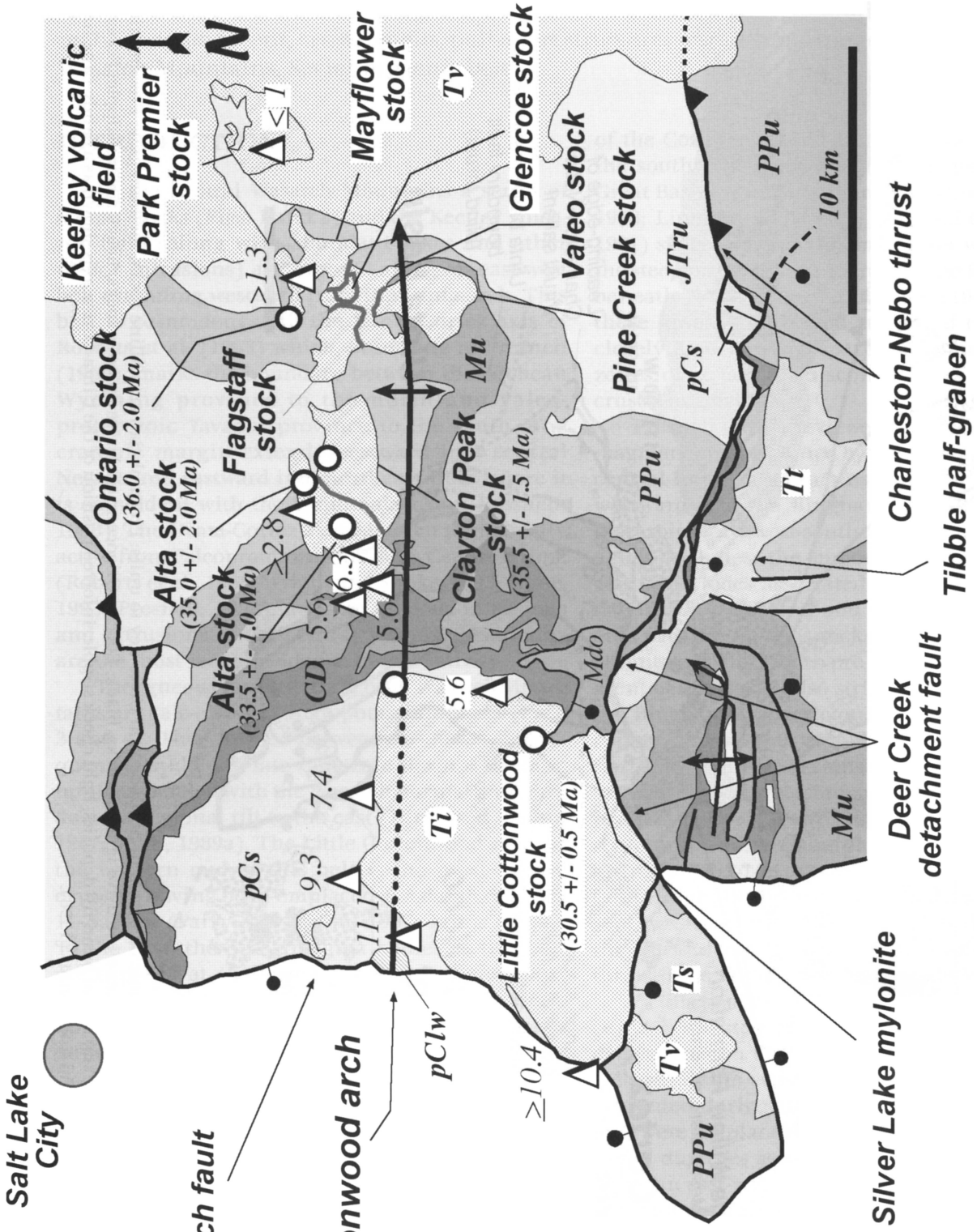

Figure 2. Geologic index map of the Wasatch igneous belt and related structural features. Emplacement ages for stocks based on U-Pb zircon analyses. Sample sites designated with open circles. Triangles denote sample sites and paleodepth determinations in kilometers (John, 1989a). Rock-unit abbreviations: pCIw, Proterozoic Little Willow Formation; pCs, Proterozoic sedimentary rocks; CD, Cambrian-Devonian undifferentiated; Mu, Mississippian undifferentiated; Mdo, Mississippian Donut Shale; PPu, Pennsylvanian-Permian undifferentiated; JTru, Jurassic-Triassic undifferentiated; Ti, late Eocene-Oligocene intrusive igneous rocks; Tt, late Eocene-Oligocene Tibble Formation; and Tv, late Eocene-Oligocene extrusive igneous rocks. Map adapted from Bryant (1992).

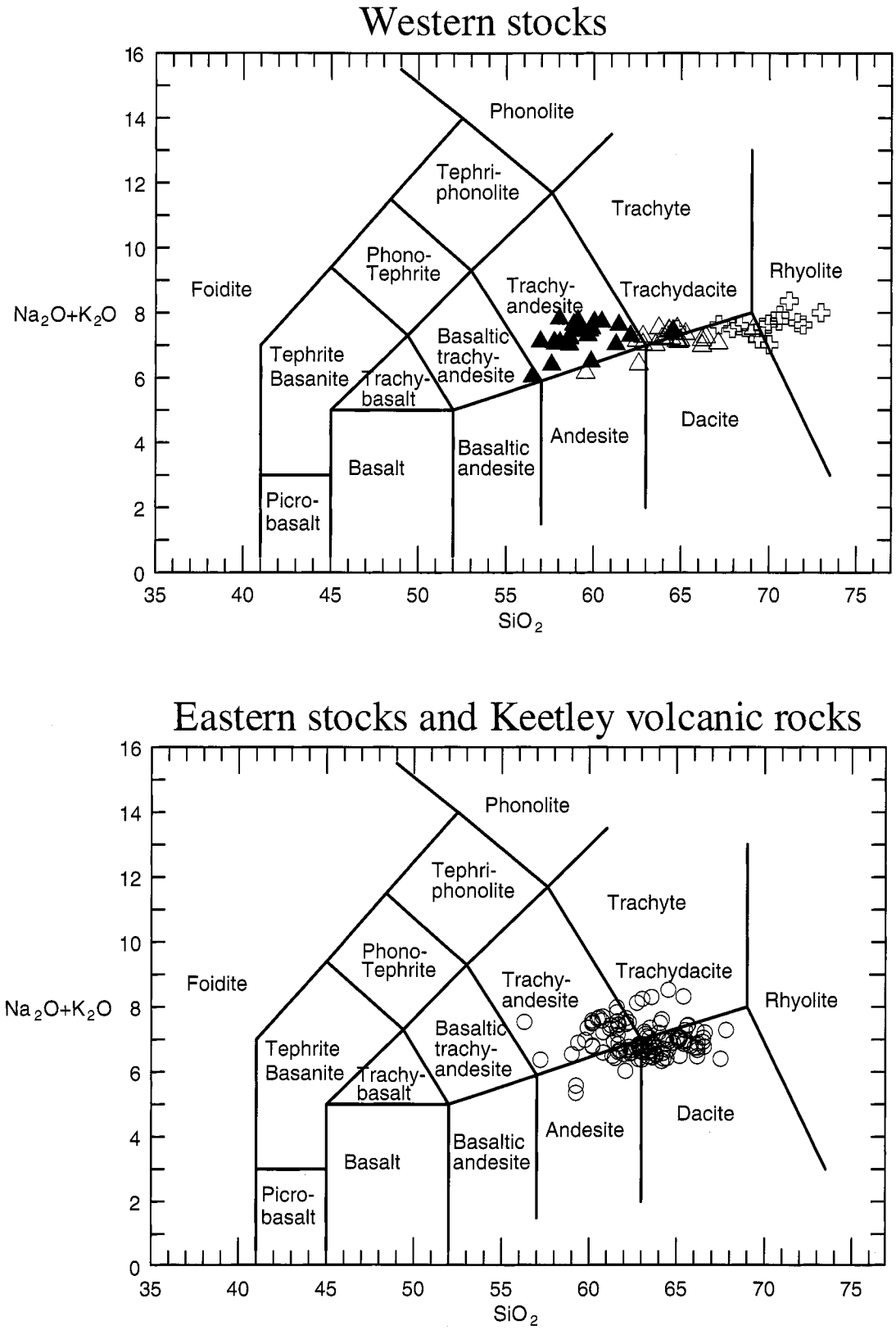

Figure 3. Classification of igneous rocks of the central Wasatch Mountains after the scheme of LeBas et al. (1986). The volcanic system was used because of the fine-grained matrix of the eastern stocks and Keetley volcanic rocks. Upper diagram key: open plus signs = Little Cottonwood stock, open triangles = Alta stock, filled triangles = Clayton Peak stock.

Mountains (Figs. 1 and 2). In Part I, we address their origin and evolution; in Part II, we address the ascent and emplacement of the magmas.

PART I. ORIGIN AND EVOLUTION OF THE IGNEOUS ROCKS IN THE CENTRAL WASATCH MOUNTAINS

General Description of the Rocks

The igneous rocks of the central Wasatch Mountains consist of two types of stocks (western and eastern) and the Keetley volcanic field (Figs. 1 and 2). The stocks are grouped based on their location and texture (John, 1989a; John et al., 1998). The western type consists of the Little Cottonwood, Alta, and Clayton Peak stocks; they are coarse-grained and mostly equigranular (Wilson, 1961; Atkin, 1982; John, 1989a; Marsh, 1992; Hanson, 1995). Each of these three stocks is compositionally distinct (Figs. 3 and 5) (Vogel et al., 1998). The eastern type consists of the Flagstaff Mountain, Ontario, Mayflower, Glencoe, Valeo, and Pine Creek stocks; they are compositionally similar to each other and to the Alta stock (Fig. 5). These stocks are generally porphyritic, characterized by coarse-grained phenocrysts in a fine- to medium-grained groundmass (John, 1989a; Hanson, 1995). To the east of the eastern stocks is the Keetley volcanic field, a sequence of lahars, debris avalanche deposits, volcanic conglomerates, air-fall tuffs, ash-flow tuffs, and minor lava flows which represent the eroded remnant of a stratavolcano (Woodfill, 1972; Leveinen, 1994; Feher, 1997). The Park Premier stock and Indian Hollow plugs intrude the Keetley volcanic field

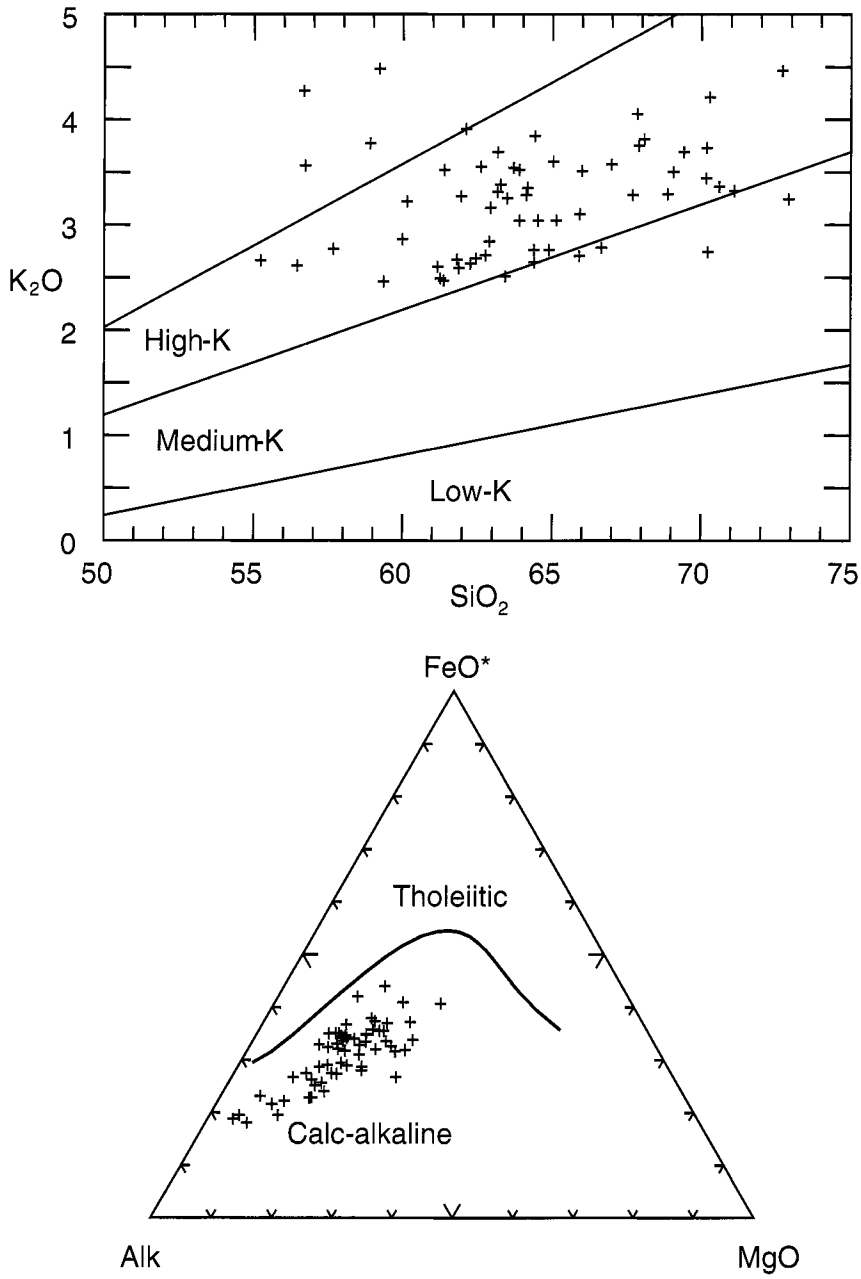

Figure 4. Igneous rocks of the central Wasatch Mountains are high-potassium rocks (upper diagram) (after Gill, 1981) and occur in the calc-alkaline field (lower diagram).

and may be its intrusive equivalents (John, 1989a, 1989b; John et al., 1998). The deposits in Keetley volcanic field extend over a 330-km^2 area between the eastern stocks and the west end of the Uinta Mountains (Bryant, 1990; Leveinen, 1994). The eastern stocks, volcanic rocks of the Keetley volcanic field, and Alta stock are chemically similar to one another but differ from the more silicic Little Cottonwood and less silicic Clayton Peak stocks (Figs. 5 and 6).

In addition to the stocks and Keetley volcanic field, the region is characterized by a set of dikes. The similarity in age and chemical composition (Fig. 5) of all

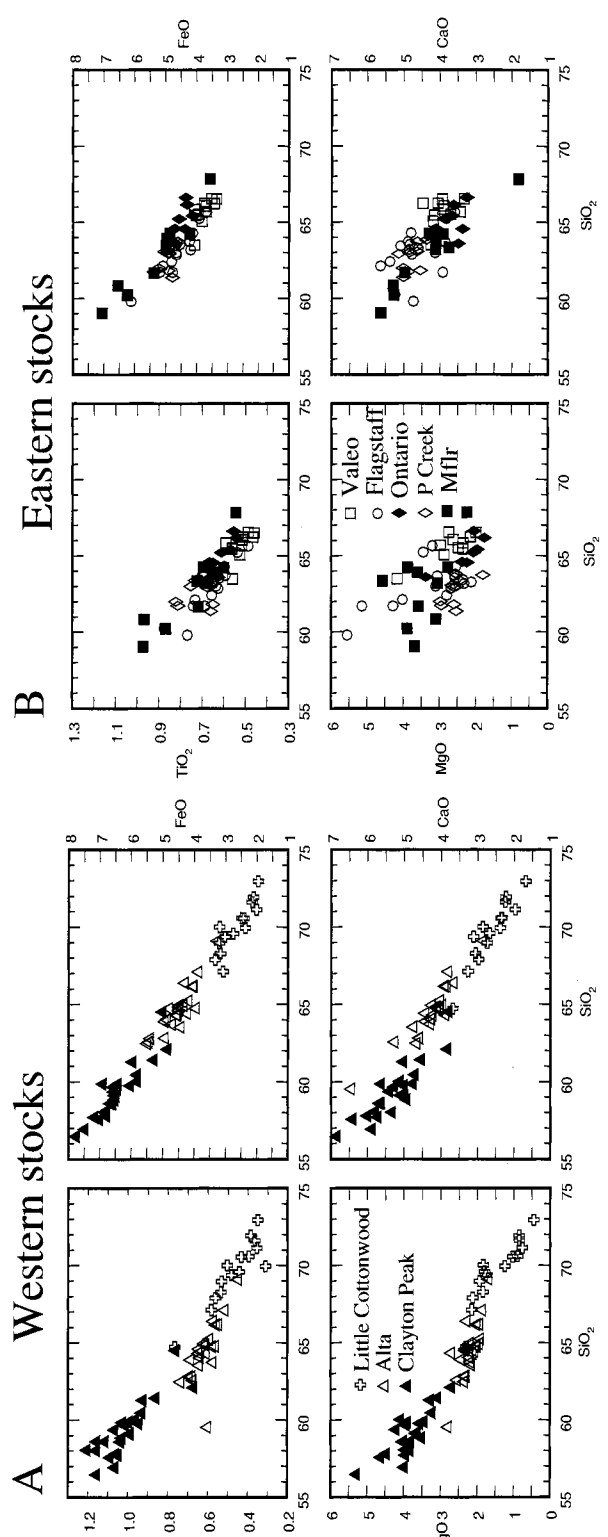

Figure 5. Variation of TiO_2, MgO, FeO, and CaO *versus* SiO_2. ***A,*** western stocks. ***B,*** eastern stocks. ***C,*** dikes. ***D,*** Keetley volcanic rocks. Symbols for dikes are the same as those for the stocks with which they are geographically associated. Note that the dikes and Clayton Peak stock have the most mafic compositions among the rocks of the Wasatch igneous belt. Most of the eastern stocks and Keetley volcanic rocks are similar to the Alta stock.

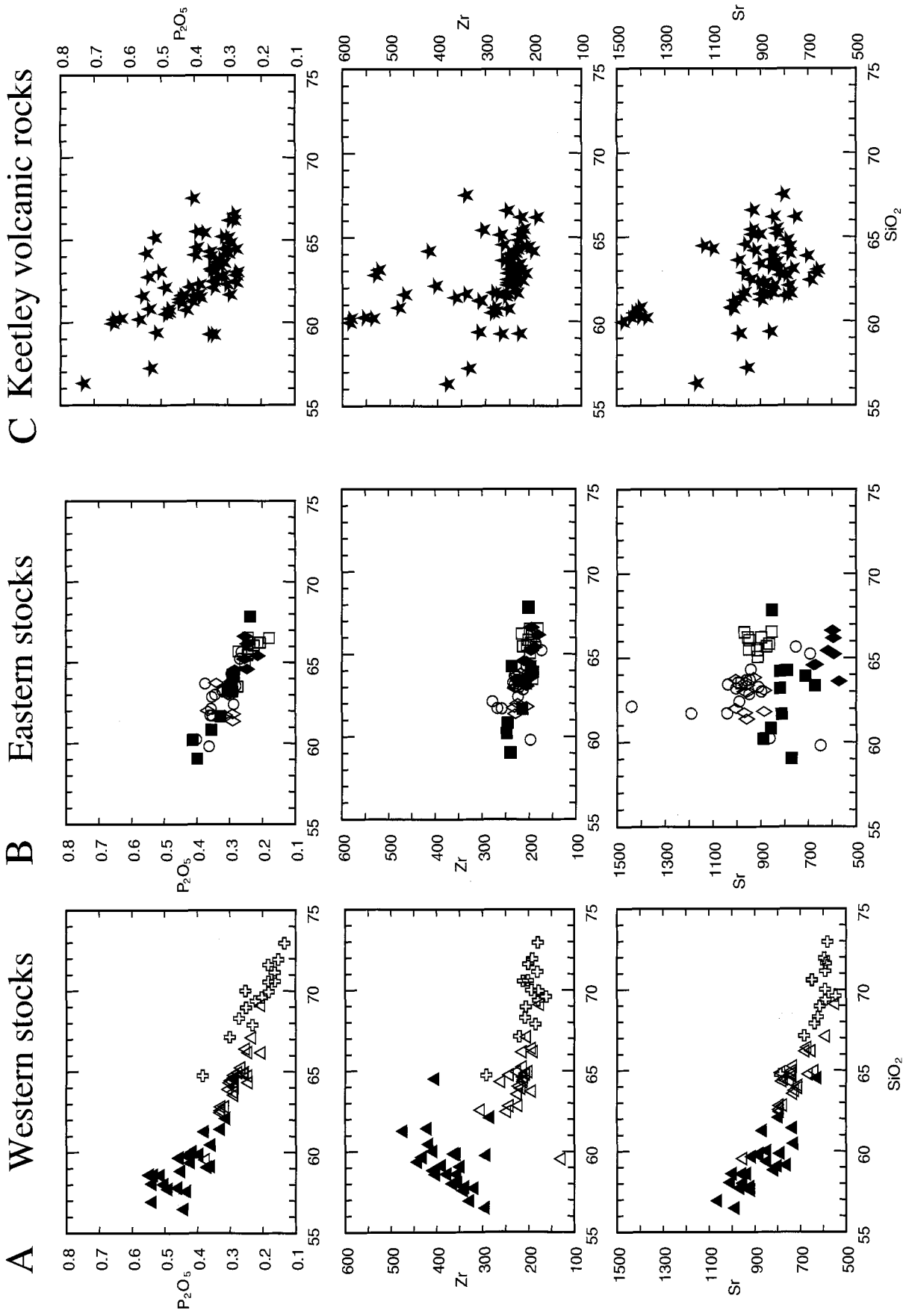

Figure 6. Variation of P_2O_5, Zr, and Sr. ***A***, western stocks; ***B***, eastern stocks; and ***C***, Keetley volcanic rocks.

these igneous rocks indicates an origin from a common source. The stocks cut some dikes but are themselves intruded by other dikes. In two locations (one in the Alta stock and the other in the Pine Creek stock) dikes have intruded the stocks and formed pillow-shaped enclaves with irregular, cuspate margins. We interpret these structures as evidence that the stocks were still molten when the dikes were intruded. Measurements of 166 dikes show a strong northeast orientation (Cambray and Holst, 1993; Vogel et al., 1998). The dikes are restricted to an area very closely associated with the belt of intrusions and volcanic deposits.

Analytical Methods

We selected fresh samples to represent the complete variation present within each unit. Major-element and selected trace element concentrations were determined by X-ray fluorescence spectrometry (XRF; Rigaku SMAX) for all samples. Additional whole-rock trace element and rare earth element concentrations were determined for selected samples, using laser ablation inductively coupled plasma mass spectrometer (LA-ICP-MS) and instrumental neutron activation analyses (INAA). The instrumental neutron activation analyses were done at the Phoenix Laboratory at the University of Michigan, and the LA-ICP-MS analyses were done at Michigan State University with a Cetac LSX-200 laser and Micromass Platform ICP-MS. Strontium and neodymium isotopes were analyzed by Damian Hodkinson and Carmela Garzione at the University of Arizona.

For whole-rock chemical analyses, we ground the samples with a ceramic flat-plate grinder, after passing them through a chipmunk crusher. We use two different techniques for preparation of glass disks: a high-dilution fusion (HDF) and low-dilution fusion (LDF). The LDF glass disks are used for LA-ICP-MS analyses. Glass disks are made by mixing the finely ground rock powder with lithium tetraborate as a flux and ammonium nitrate as an oxidizer. The proportion for HDF is 1 gm rock, 9 gm lithium tetraborate, and 0.25 gm ammonium nitrate; for LDF these proportions were 3:9:0.50, respectively. These materials are mixed and fused at 1000°C in a platinum crucible for at least 30 minutes and then poured into platinum molds. The glass disks were analyzed by XRF and LA-ICP-MS methods. The precision and accuracy of these methods are discussed in Mills et al. (1997) and Hannah et al. (2001).

In our laboratory XRF major element analyses are reduced by the fundamental parameter data reduction method (Criss, 1980) using XRFWIN software (Omni Instruments). XRF trace element analyses are reduced by standard linear regression techniques. For LA-ICP-MS data reduction, strontium (determined from XRF analyses) is used as the internal standard. Prior to any calculation the background signal is subtracted from standards and samples. The concentration of the REE in the samples is calculated based on linear regression techniques using BHVO-1, W-2, JB-2, JA-3, BIR-1 standards.

Mineralogy of the Stocks

The mineralogy of the stocks has been described and summarized by John (1989a) and Hanson (1995). Detailed descriptions of the mineralogy of individual stocks can be found in the following references. For the Little Cottonwood stock, see Lawton (1980); Marsh (1992); and Marsh and Smith (1997). For the Alta stock, see Wilson (1961) and John (1992). For the Clayton Peak stock, see Palmer (1974) and Atkin (1982). For the eastern stocks, see Scales (1972); Bromfield et al. (1977); and John (1989a). For the Keetley volcanic rocks, see Woodfill (1972); Leveinen (1994); and Feher (1997). The following descriptions are modified from these authors. The rock classification terminology is from Streckeisen (1976).

The Little Cottonwood stock ranges in rock type from granite to granodiorite. The stock varies from equal proportions of plagioclase, K-feldspar, and quartz to dominantly plagioclase and quartz. K-feldspar commonly occurs as megacrysts that range from 2–6 cm in size. Orthoclase is the most common alkali feldspar, although microcline is present in some samples (Hanson, 1995). Biotite is the most abundant mafic phase with hornblende being less abundant. Accessory minerals are magnetite, sphene, zircon, apatite and allanite.

The Alta stock ranges in rock type from granodiorite to quartz monzonite. It is dominated by plagioclase with lesser amounts of quartz and K-feldspar. Biotite and hornblende are the mafic phases; clinopyroxene occurs as inclusions in some plagioclase grains. Magnetite, ilmenite, sphene, zircon, and apatite are present as accessory phases.

The Clayton Peak stock ranges in rock type from quartz monzodiorite to quartz monzonite with clinopyroxene, orthopyroxene, and biotite as the most abundant mafic phases; generally, hornblende is not abundant but commonly occurs as overgrowths on pyroxenes. Biotite occurs as individual grains and as overgrowths on hornblende. K-feldspar is more abundant than quartz. Magne-

tite, sphene, zircon and apatite are present as accessory phases. Towards the margin of the stock, hornblende becomes more abundant, and quartz and pyroxene decrease in abundance.

Igneous rocks of the eastern stocks and Keetley volcanic field are all porphyritic. Phenocryst content in the eastern stocks ranges from 35–55%. The phenocrysts are plagioclase, hornblende, biotite and in some stocks, quartz (Hanson, 1995). Quartz content ranges from zero in Pine Creek and Ontario stocks to abundant in Glencoe stock. Quartz generally has resorption textures. Magnetite and ilmenite are present as accessory phases.

The rocks from the Keetley volcanic field range in phenocryst content from 35–60% (Leveinen, 1994; Feher, 1997); plagioclase, hornblende, augite, and biotite are the dominant phenocryts. Quartz and orthopyroxene occur but are not common. Augite generally occurs as reaction rims around hornblende phenocrysts. Biotite is present in all stocks but is commonly altered to chlorite and magnetite. Accessory minerals are magnetite, ilmenite, zircon, and apatite. Alteration is much more pervasive in the eastern stocks and Keetley volcanic field than in the western stocks.

Because the matrices of the eastern stocks and the Keetley volcanic rocks are too fine grained to be point counted, the chemical classification system for volcanic rocks of LeBas et al. (1986) is used. For comparison purposes this same classification is also used for the western stocks in Figure 3. The compositional variation of western and eastern stocks falls along the boundary between andesite and trachy-andesite, and dacite and trachydacite. The Little Cottonwood stock has a higher silica content and extends into the rhyolite field. The Clayton Peak stock is in the trachyandesite field and is the most mafic stock. The compositional variations within the Keetley volcanic rocks are very similar to those of the eastern stocks with the trend occurring slightly across the boundary from the trachyandesite field into the dacite field.

Dikes associated with this belt are porphyritic with a fine-grained matrix. Phenocrysts of the dikes are similar to those of the eastern stocks. Most consist of plagioclase, hornblende, and biotite; some contain quartz, and orthoclase is scarce. Alteration of the dikes is common, and altered dikes were avoided for chemical analyses.

Petrochemistry of the Stocks

Igneous rocks of the central Wasatch Mountains (Fig. 2) belong to the high-potassium, calc-alkaline series (Fig. 4). The range of rock types as well as major- and trace element signatures (e.g., Nb and Ti depletion) (Fig. 4) are similar to other calc-alkaline rocks generally assumed to be generated by contemporaneous subduction-related processes. In this respect these rocks are similar to other calc-alkaline rocks that occur in the Great Basin (Barr, 1993). However, recent work on the Colville igneous complex in northeastern Washington by Morris et al. (2000) questions the assumption that calc-alkaline rocks such as these are derived from subduction-zone processes. Their conclusion is based on key major-, trace-, and rare earth element data that are not consistent with large-scale fractionation that would be required to produce the compositional variation observed in the Colville igneous complex. In this respect, the Colville igneous complex is similar to the igneous rocks of the central Wasatch Mountains.

Representative analyses for all stocks and the Keetley volcanic rocks are shown in Tables 1, 2, and 3. The western stocks (Little Cottonwood, Alta, and Clayton Peak stocks) are compositionally distinct from one another (Figs. 5 and 6). The Clayton Peak stock is the most mafic, the Alta stock is intermediate, and the Little Cottonwood stock is the least mafic. The statistical means and standard deviations of SiO_2 wt. % in these stocks are 58.8 $\pm$ 1.9; 64.6 $\pm$ 1.7; and 69.5 $\pm$ 1.9, respectively. There is a general linear variation of all the major elements with respect to silica for the western stocks (Figs. 5 and 6). These stocks form a continuous variation from low silica to high silica with very little compositional overlap among the stocks.

The eastern stocks and Keetley volcanic rocks are chemically similar to each other and to the Alta stock (Feher, 1997) (Figs. 4 and 5). Major element variations within the eastern stocks and Keetley volcanic rocks are in general similar. The scatter in major element data for the Keetley volcanic rocks is larger than that in the eastern stocks, and is particularly striking in the variation of TiO_2 and MgO (Fig. 5). There is a relatively large variation in some trace elements in the Keetley volcanic rocks as compared to the eastern stocks. For example, the Zr range in the eastern stocks is about 100 ppm, whereas the Zr range in the Keetley volcanic rocks is about 300 ppm (Fig. 6). Such large compositional variations in the volcanic rocks as compared to the stocks probably indicate that the volcanic rocks sampled a wide variety of magma reservoirs, whereas a stock represents the crystallization one magmatic body, although it may have formed by the coalescence of multiple batches of magma.

Table 1 (Continued on p. 142-144). Selected major element analyses.

Sample	SiO_2	TiO_2	Al_2O_3	FeO	MnO	MgO	CaO	Na_2O	K_2O	P_2O_5	Totals
Flagstaff stock											
TF-1	63.35	0.62	16.74	4.52	0.09	2.57	4.81	4.00	2.72	0.28	99.70
TF-2	63.20	0.65	17.74	4.19	0.10	2.31	4.85	4.16	2.49	0.32	100.01
TF-3	62.77	0.65	16.79	4.85	0.08	2.10	4.57	4.38	2.71	0.32	99.22
TBON-1	59.20	0.76	15.43	6.05	0.11	5.50	4.69	4.08	2.81	0.36	98.99
F7-2	59.36	0.70	15.23	4.86	0.09	3.84	5.39	3.28	2.46	0.34	95.55
F7-3	60.93	0.64	16.63	4.69	0.09	2.73	5.25	3.92	2.47	0.28	97.63
F7-4	60.00	0.72	15.38	5.04	0.09	4.16	4.83	3.79	2.86	0.35	97.22
TF930703-4V	62.28	0.63	16.99	4.61	0.09	3.07	4.09	4.13	2.63	0.34	98.86
TF930705-1	62.87	0.62	16.84	4.57	0.09	3.02	3.80	4.00	2.54	0.37	98.72
TF930707-1	64.79	0.48	15.45	3.65	0.07	3.15	3.54	4.32	2.98	0.26	98.69
TF930707-5	61.06	0.68	15.74	4.72	0.09	5.09	3.88	4.21	3.13	0.35	98.95
TF930707-7B	63.44	0.59	16.35	4.07	0.08	2.51	4.74	4.08	2.51	0.29	98.66
TF930707-7C	63.19	0.52	15.16	3.79	0.08	3.34	3.71	3.83	2.99	0.26	96.87
TF930707-16	62.24	0.58	16.40	4.13	0.08	2.52	4.77	4.15	2.52	0.29	97.68
TF930708-5V	62.21	0.62	16.99	4.60	0.10	2.66	4.73	4.15	2.55	0.35	98.96
TF930705-3	59.84	0.87	16.11	6.20	0.11	3.86	5.21	3.66	3.08	0.40	99.34
Mayflower stock											
M8-10	59.75	0.95	15.94	6.42	0.11	3.04	5.20	3.40	3.05	0.35	98.21
M8-11	65.93	0.53	15.96	3.46	0.06	2.18	1.76	3.96	3.10	0.23	97.17
M10-6	57.68	0.95	16.18	6.88	0.13	3.60	5.50	3.60	2.77	0.39	97.68
TM930711-1	59.62	0.86	16.07	6.17	0.11	3.85	5.22	3.63	3.06	0.41	99.00
TM930710-4	62.14	0.71	14.84	4.88	0.10	4.49	3.68	3.43	3.50	0.30	98.07
TM930710-10	63.05	0.59	15.93	4.14	0.07	3.81	3.85	3.62	2.81	0.28	98.15
TM930710-11	63.50	0.65	15.51	4.94	0.09	3.59	4.08	3.44	3.25	0.29	99.34
TM930710-12	60.15	0.70	15.73	5.24	0.10	3.49	4.85	3.72	3.22	0.32	97.52
Ontario stock											
O11-3	64.42	0.56	15.45	4.04	0.08	1.92	3.60	4.33	3.84	0.21	98.45
O11-4	63.02	0.65	15.90	4.59	0.09	2.30	4.01	3.42	3.33	0.24	97.55
O11-5	63.72	0.64	15.75	4.32	0.07	2.20	3.32	4.85	3.54	0.28	98.69
O18-1	66.02	0.55	15.52	4.30	0.08	2.02	3.22	3.61	3.51	0.25	99.08
O18-2	65.04	0.53	15.76	4.22	0.09	1.72	3.55	3.53	3.60	0.24	98.28
O18-3	64.18	0.60	16.09	4.48	0.09	2.02	3.80	3.54	3.35	0.25	98.40

The dikes have a much more restricted compositional variation than do either the stocks or Keetley volcanic rocks. Most dike samples vary between 55–63 wt. % SiO_2. The compositional variation in the dike samples is similar to that in the Clayton Peak stock (Fig. 5), which is the least evolved of the igneous bodies in the area.

Patterns for the spider and rare earth element (REE) diagrams for the samples from the stocks and Keetley volcanic rocks are similar (Figs. 7 and 8). The chondrite-normalized spider diagrams display the classic subduction-related pattern of relatively enriched large ion lithophile elements (Rb, Ba, Th) with relatively depleted high-field strength elements (Ta, Nb and Ti) (Fig. 7). Patterns for chondrite-normalized REEs for all of the stocks and Keetley volcanic rocks are similar, showing a nearly constant slope (Fig. 8), even though they have a large range in major element compositions (55–75 wt. % SiO_2). The REEs are light element enriched, with no significant Eu anomaly (Fig. 8); Eu/Eu* values show little variation. There is no systematic variation of Eu/Eu* with Al_2O_3 or Sr variation, and this lack of variation would preclude the fractionation of plagioclase as the major control in the compositional variation in these rocks. In Figure 9 the REEs are normalized to the most mafic sample of the Clayton Peak stock. In most samples, there is a decrease in REEs (Figs. 9 and 10). There is a small decrease in the middle REEs with increase in silica content (except for the most

Table 1 (Continued).

Sample	SiO_2	TiO_2	Al_2O_3	FeO	MnO	MgO	CaO	Na_2O	K_2O	P_2O_5	Totals
Pine Creek stock											
To930718-9	63.90	0.63	15.60	4.70	0.10	3.39	3.50	4.80	3.52	0.30	100.44
P5-9	63.15	0.68	16.57	4.83	0.09	2.52	4.32	3.95	2.51	0.29	98.91
P5-10	61.83	0.65	16.47	4.92	0.08	2.59	4.54	3.97	2.67	0.29	98.01
P5-12	61.38	0.66	16.32	4.77	0.09	2.53	5.00	4.00	2.47	0.29	97.51
P6-8	61.71	0.71	16.64	4.63	0.08	2.36	4.53	3.83	2.56	0.29	97.34
P6-9	62.12	0.74	16.73	4.83	0.09	2.48	4.77	3.96	2.57	0.30	98.59
P6-12	61.18	0.81	16.76	5.14	0.10	2.93	4.94	3.84	2.60	0.36	98.66
P6-14	60.95	0.80	16.96	5.30	0.11	2.90	4.81	3.93	2.62	0.31	98.69
P9-2	61.89	0.67	16.90	4.45	0.08	1.74	4.49	3.95	2.59	0.33	97.09
TPC93705-10	61.83	0.65	16.47	4.92	0.08	2.59	4.54	3.97	2.67	0.29	98.01
TPC93705-12	61.38	0.66	16.32	4.77	0.09	2.53	5.00	4.00	2.47	0.29	97.51
Valeo stock											
TV-1	66.65	0.46	16.62	3.36	0.08	1.99	3.94	4.13	2.78	0.18	100.19
V7-2V	64.74	0.58	15.86	3.99	0.09	2.30	3.85	3.89	2.78	0.24	98.32
V7-3V	64.39	0.55	15.94	3.88	0.07	2.43	3.64	4.37	2.76	0.24	98.27
V10-1V	64.13	0.55	15.90	3.93	0.08	2.30	4.06	4.03	2.74	0.24	97.96
V10-2V	64.89	0.50	15.82	3.67	0.09	2.10	3.97	3.96	2.76	0.21	97.97
V7-10	64.39	0.50	15.78	3.60	0.07	2.55	3.79	3.93	2.63	0.22	97.46
TV930707-9	62.46	0.55	15.79	4.00	0.08	4.10	4.18	4.24	2.68	0.27	98.35
TV930709-1V	65.64	0.48	15.83	3.46	0.07	2.70	3.28	4.06	2.87	0.24	98.63
TV930709-2V	64.90	0.51	15.70	3.63	0.13	2.94	3.39	4.36	2.97	0.27	98.80
TV930705-2	64.40	0.52	16.00	3.79	0.09	2.84	4.14	4.31	2.64	0.25	98.98
Little Cottonwood stock											
072095-6	67.72	0.56	15.30	3.31	0.05	2.11	2.96	3.91	3.58	0.23	99.73
072095-8	70.29	0.35	15.02	1.98	0.04	0.75	1.94	4.05	4.21	0.16	98.79
072095-9	70.19	0.43	15.15	2.40	0.04	1.02	2.34	4.26	3.44	0.18	99.45
072095-11	69.98	0.39	15.03	2.45	0.04	0.88	2.31	4.21	3.65	0.16	99.10
072095-14	71.19	0.38	14.54	2.07	0.04	0.83	2.20	4.19	3.35	0.15	98.94
072095-15	70.92	0.36	14.72	2.12	0.04	0.83	2.21	3.96	3.66	0.18	99.00
071895-4B	70.24	0.28	15.34	2.15	0.04	1.25	2.26	4.93	2.74	0.11	99.34
072095-16	69.43	0.44	14.90	2.74	0.05	1.79	2.66	3.84	3.69	0.20	99.74
950720-LC-1	69.85	0.31	15.85	2.36	0.04	1.23	2.38	4.97	2.67	0.18	99.84
950720-LC-2	67.73	0.42	15.85	2.46	0.05	1.71	2.90	4.03	4.05	0.20	99.40
950720-LC-2A	69.72	0.50	14.25	3.09	0.06	2.14	3.01	3.83	3.20	0.22	100.02
950720-LC-4	70.62	0.41	14.39	2.64	0.06	1.76	2.66	3.82	3.36	0.17	99.89
950720-LC-5	69.69	0.50	14.23	3.17	0.05	1.82	2.84	3.89	3.09	0.25	99.53
950720-LC-6	67.91	0.53	15.11	3.14	0.05	1.83	3.03	3.80	3.75	0.27	99.42
950720-LC-7	69.24	0.48	14.77	3.01	0.04	1.76	3.10	3.91	3.27	0.22	99.80
950720-LC-8	68.89	0.53	14.96	3.19	0.05	1.93	2.73	4.06	3.29	0.25	99.88

Table 1 (Continued).

Sample	SiO_2	TiO_2	Al_2O_3	FeO	MnO	MgO	CaO	Na_2O	K_2O	P_2O_5	Totals
Clayton Peak stock											
CP92-2	57.24	1.07	16.96	7.52	0.12	4.00	5.91	3.62	3.53	0.54	100.51
CP92-3	58.95	1.03	16.99	6.53	0.11	3.52	4.93	3.63	4.02	0.45	100.16
CP92-4	59.36	0.99	16.73	6.55	0.11	3.68	5.11	3.60	3.87	0.36	100.36
CP92-5	61.14	0.94	16.87	5.88	0.10	3.26	4.76	3.79	4.01	0.36	101.11
CP92-6A	58.33	1.21	16.48	6.87	0.11	3.97	5.82	3.43	3.69	0.54	100.45
CP92-6B	59.38	1.17	16.69	6.70	0.11	3.86	5.74	3.46	3.65	0.54	101.30
TCP-2	62.15	0.87	16.95	5.34	0.10	3.11	4.59	3.60	4.11	0.33	101.15
TCP-3	59.30	0.99	16.63	6.51	0.11	3.64	5.01	3.74	4.05	0.37	100.35
C12-21	56.68	1.13	16.04	6.63	0.12	3.74	5.20	3.36	4.27	0.49	97.66
C13-9	58.91	0.93	16.48	5.94	0.10	3.51	4.93	3.57	3.77	0.42	98.56
C13-12	56.73	1.04	15.95	6.66	0.11	4.39	5.89	3.35	3.56	0.45	98.13
C13-15	57.21	1.01	15.72	6.50	0.11	3.93	5.54	3.50	3.59	0.50	97.61
C13-18	58.04	1.04	15.08	6.39	0.11	4.11	5.27	3.19	4.10	0.41	97.74
C14-1	56.73	1.03	16.37	7.05	0.12	3.88	5.62	3.44	3.53	0.48	98.25
C14-4	60.30	0.91	15.77	5.86	0.10	3.23	4.94	3.47	3.44	0.37	98.39
C14-12	58.89	1.01	15.41	6.79	0.11	3.83	5.53	3.37	3.02	0.42	98.38
C15-3	56.08	1.06	15.91	6.83	0.11	4.50	6.24	3.40	2.83	0.42	97.38
C15-5	55.23	1.13	15.51	7.58	0.13	5.17	6.69	3.24	2.66	0.43	97.77
TC15-11	62.12	0.67	16.15	4.85	0.09	2.70	3.82	3.38	3.91	0.31	98.00
TCP-1	60.77	1.01	16.73	6.51	0.10	3.50	4.83	3.49	4.14	0.40	101.48
93713-1	63.61	0.75	15.56	4.93	0.08	2.30	3.73	3.55	3.79	0.28	98.58
93713-14	57.95	1.10	16.01	6.52	0.10	3.95	5.56	3.49	3.64	0.54	98.86
93713-17	59.31	0.95	15.57	5.74	0.10	4.03	5.05	3.46	4.16	0.41	98.78
93715-13	58.22	0.64	14.81	4.98	0.12	4.30	8.38	3.06	2.72	0.41	97.64
TC93-15	59.05	1.00	15.54	6.48	0.11	3.88	5.21	3.35	3.88	0.45	98.95
Alta stock											
TALT-1	66.09	0.57	15.16	4.27	0.07	2.27	3.63	3.63	3.58	0.25	99.52
TALT-2	63.78	0.64	16.00	4.51	0.08	2.68	3.84	3.76	3.60	0.24	99.13
TALT-3	64.50	0.61	16.43	4.53	0.09	2.12	4.23	3.80	3.67	0.30	100.28
TALT-4	60.41	0.61	17.79	6.53	0.11	2.83	6.54	4.05	2.19	0.38	101.44
A92-1	65.72	0.62	16.53	4.54	0.08	2.22	4.16	3.84	3.35	0.26	101.32
A12-7	67.86	0.44	14.61	3.20	0.06	1.65	2.79	3.32	4.05	0.20	98.18
A12-11	63.19	0.63	15.82	4.38	0.07	2.26	3.95	3.50	3.69	0.28	97.77
A19-5	61.27	0.66	16.31	5.32	0.09	2.49	5.15	3.79	2.49	0.32	97.89
A19-8	62.24	0.63	16.74	4.33	0.09	2.11	4.65	3.98	2.88	0.28	97.93
A20-5	62.90	0.62	16.24	4.11	0.09	2.01	4.32	3.82	3.21	0.29	97.61
A20-10	65.19	0.55	15.70	3.98	0.07	1.98	3.78	3.57	3.48	0.20	98.50
A20-13	61.11	0.72	16.35	5.37	0.10	2.30	4.56	3.86	3.12	0.32	97.81
A20-15	61.72	0.68	16.47	5.29	0.10	2.26	4.50	3.67	3.23	0.32	98.24
A22-3	64.14	0.61	16.08	4.41	0.08	1.92	4.19	3.77	3.28	0.27	98.75
A22-5	64.06	0.58	16.07	4.10	0.08	1.87	3.94	3.69	3.52	0.26	98.17
93719-16	62.10	0.56	16.19	4.58	0.09	2.12	4.18	4.02	3.31	0.28	97.43
93719-17	65.35	0.54	15.93	3.94	0.07	1.91	3.85	3.78	3.11	0.24	98.72
93719-18	63.90	0.57	16.13	4.72	0.08	1.97	4.04	3.99	3.04	0.24	98.68
93719-23	63.28	0.68	15.87	4.87	0.10	2.41	4.38	3.73	3.38	0.30	99.00
93720-4	62.02	0.67	16.74	4.86	0.10	2.30	4.53	3.99	3.18	0.31	98.70
93720-9	66.45	0.51	15.33	3.82	0.08	1.84	3.76	3.66	3.33	0.23	99.01
93720-11	63.43	0.55	16.45	3.85	0.09	1.98	3.93	4.01	3.34	0.28	97.91
93720-12	64.15	0.61	16.23	4.28	0.09	2.17	3.91	3.80	3.27	0.25	98.76
93722-8	63.18	0.63	16.16	4.80	0.09	2.18	4.20	3.81	3.31	0.28	98.64

Table 1 (Continued).

Sample	SiO_2	TiO_2	Al_2O_3	FeO	MnO	MgO	CaO	Na_2O	K_2O	P_2O_5	Totals
Keetley volcanic rocks											
TK18-10	63.71	0.66	15.66	4.82	0.08	1.87	4.88	3.67	3.21	0.27	98.83
15-5 I-80	61.11	0.86	15.17	5.06	0.10	4.59	5.24	3.37	3.52	0.44	99.46
15-9 I-80	62.70	0.63	16.57	4.51	0.09	3.19	4.92	3.93	2.87	0.31	99.72
15-11 I-80	67.15	0.77	13.29	4.03	0.07	3.39	3.98	3.07	3.27	0.40	99.42
15-14 I-80	61.40	0.68	17.06	4.89	0.09	3.29	5.25	4.21	2.35	0.29	99.51
15-15 I-80	63.82	0.59	16.74	4.19	0.08	2.97	4.68	4.31	2.60	0.31	100.29
20-14 I-80	62.27	0.67	16.30	4.82	0.09	3.50	5.08	3.92	2.63	0.34	99.62
20-17 I-80	63.03	0.69	17.09	4.54	0.05	2.14	4.92	4.12	2.45	0.32	99.35
20-18 I-80	65.63	0.60	15.70	3.90	0.05	1.92	4.63	3.82	2.58	0.29	99.12
20-19 I-80	64.60	0.86	17.55	3.80	0.04	1.29	4.87	3.93	2.72	0.39	100.05
20-3 FRAN	61.70	0.70	15.90	5.30	0.10	3.65	4.62	3.27	3.30	0.27	98.81
20-4 FRAN*	63.19	0.70	15.96	5.32	0.09	3.57	4.71	3.25	3.12	0.27	100.18
20-6 FRAN	64.11	0.75	16.48	5.26	0.05	2.03	4.85	3.73	2.78	0.32	100.36
20-11 FRAN	62.36	0.70	15.77	5.23	0.10	3.59	4.84	3.18	3.14	0.27	99.18
20-13 FRAN	64.20	0.58	15.94	4.66	0.09	2.73	4.52	3.82	3.38	0.35	100.27
18-12 PEO	63.35	1.03	14.45	4.46	0.12	4.40	4.38	3.19	4.99	0.54	100.91
18-14 PEO	62.57	0.76	15.64	4.99	0.09	3.40	4.81	2.94	3.58	0.34	99.12
19-27 PEO	61.37	0.85	16.19	6.03	0.10	3.23	5.22	3.19	3.20	0.38	99.76
19-28 PEO	61.78	0.78	15.53	5.36	0.14	3.86	5.05	3.20	3.41	0.34	99.45
19-31 PEO	61.38	0.93	14.40	4.76	0.12	4.47	4.70	2.99	4.55	0.48	98.78
17-28 JD	61.39	0.69	16.41	5.25	0.11	2.76	4.81	3.93	3.85	0.43	99.63
18-8 JD*	56.27	0.86	18.11	6.90	0.14	2.99	6.26	3.64	2.60	0.52	98.29
18-9A JD	60.90	0.70	16.76	5.63	0.11	2.74	4.90	3.80	3.48	0.44	99.46
18-9B JD	60.55	0.69	16.68	5.50	0.11	2.81	4.74	3.61	3.71	0.40	98.80
19-1 JD*	63.94	0.87	14.55	4.83	0.07	2.63	4.59	3.34	4.22	0.54	99.58
19-2 JD	59.28	0.73	18.50	5.51	0.11	4.00	6.21	3.87	1.46	0.34	100.01
19-3B JD	63.72	0.65	16.66	4.26	0.07	3.07	4.89	3.56	2.87	0.33	100.08
19-7 JD*	64.89	0.65	16.18	4.53	0.05	2.24	4.38	3.79	3.08	0.29	100.08
19-13 JD	62.03	0.66	16.23	4.76	0.10	3.71	5.02	3.27	3.44	0.30	99.52
19-16 JD	65.68	0.81	14.34	5.28	0.08	2.39	4.53	3.85	3.01	0.37	100.34
19-25 JD	59.21	0.85	17.03	6.63	0.12	2.73	5.75	3.61	3.24	0.51	99.68
19-32 JD	64.18	0.64	15.83	4.81	0.07	2.74	4.81	3.91	2.46	0.35	99.80
19-33 JD	63.52	0.70	16.40	5.03	0.06	2.82	4.72	4.10	2.75	0.35	100.45
19-37 JD*	67.07	0.53	16.18	3.90	0.05	1.86	4.03	4.07	2.73	0.28	100.70
19-4 JD	64.58	0.64	16.42	4.74	0.06	1.51	4.36	3.91	2.49	0.31	99.02
19-9 JD	59.39	1.06	14.26	5.03	0.09	5.32	5.40	2.80	4.59	0.61	98.55
19-10 JD*	59.29	1.06	14.10	5.40	0.08	4.91	5.56	2.98	4.46	0.63	98.47
19-17 JD	64.39	0.74	16.63	4.46	0.02	0.79	4.34	3.77	3.16	0.51	98.81
Indian Hollow											
16-04 IH	65.32	0.63	15.00	4.62	0.06	2.46	4.29	3.71	3.22	0.39	99.70
16-09(*) IH	63.29	0.61	15.68	4.47	0.06	2.44	4.40	3.92	3.47	0.39	98.73
16-08 IH	61.55	0.65	16.39	5.20	0.10	3.21	5.07	3.76	3.53	0.40	99.86
16-10 IH	61.87	0.62	16.18	4.82	0.09	2.99	4.89	3.77	3.68	0.38	99.29
16-13 IH	60.49	0.68	16.21	5.45	0.10	3.34	5.33	3.87	3.65	0.42	99.54
17-2 IH	63.42	0.56	16.18	4.56	0.10	2.98	4.38	3.76	3.56	0.33	99.83
17-13 IH	56.28	0.98	18.09	7.00	0.10	2.46	6.77	4.09	3.42	0.73	99.92
17-23 IH	60.01	0.73	16.45	5.81	0.11	3.00	5.01	3.81	3.74	0.48	99.15
17-24 IH	59.93	0.72	16.26	5.63	0.11	3.09	5.10	3.86	3.70	0.47	98.87
17-25 IH	60.20	0.70	16.25	5.55	0.11	2.99	5.09	3.89	3.71	0.47	98.96
17-31 IH	61.89	0.66	16.31	5.22	0.10	2.78	4.76	3.74	3.68	0.41	99.55

Table 2 (Continued on p. 146-148). Selected XRF trace element analyses.

Sample	Zn	Rb	Sr	Y	Zr	Nb	Ba
Flagstaff stock							
TF-1	73	58	996	22	205	BD	1701
TF-2	73	51	1004	22	230	BD	1812
TF-3	57	61	910	26	234	BD	1864
TBON-1	86	62	650	27	198	10	1707
F7-2	63	57	1439	14	278	BD	3258
F7-3	73	57	990	20	224	BD	1762
F7-4	74	69	1042	27	267	BD	2158
TF930703-4V	127	61	898	17	221	BD	2054
TF930705-1	79	57	961	18	231	BD	2052
TF930707-1	57	70	754	19	186	BD	1875
TF930707-5	68	65	1191	28	258	BD	3146
TF930707-7B	72	61	942	20	206	BD	1717
TF930707-7C	57	74	694	16	173	BD	1728
TF930707-16	77	64	947	22	205	BD	1651
TF930708-5V	68	60	948	20	213	BD	1706
TF930705-3	81	96	864	27	249	BD	1645
Mayflower stock							
M8-10	129	81	859	26	246	10	1946
M8-11	58	83	853	16	201	BD	2042
M10-6	99	81	771	33	240	13	1850
TM930711-1	77	89	890	26	248	BD	1716
TM930710-4	60	94	673	27	221	BD	1789
TM930710-10	64	68	819	18	197	BD	1755
TM930710-11	73	86	712	23	191	BD	1849
TM930710-12	79	84	813	21	214	BD	1794
Ontario stock							
O11-3	81	144	617	12	188	8	1266
O11-4	86	123	669	17	211	11	1441
O11-5	77	104	676	14	206	12	1679
O18-1	87	119	598	20	195	BD	1433
O18-2	73	117	594	14	181	BD	1396
O18-3	93	104	593	16	196	BD	1418
Pine Creek stock							
To930718-9	57	111	570	19	195	BD	1222
P5-9	79	59	929	20	218	BD	2109
P5-10	60	58	886	15	205	BD	1980
P5-12	72	66	960	28	229	BD	1851
P6-8	72	69	959	17	223	BD	2144
P6-9	73	66	966	22	228	BD	2203
P6-12	79	64	1004	25	224	BD	2357
P6-14	120	62	969	25	231	BD	2044
P9-2	84	68	1005	20	225	BD	2271
TPC93705-10	60	58	886	15	205	BD	1980
TPC93705-12	72	66	960	28	229	BD	1851

Table 2 (Continued).

Sample	Zn	Rb	Sr	Y	Zr	Nb	Ba
Valeo stock							
TV-1	78	76	969	12	198	BD	2013
V7-2V	100	65	864	16	201	BD	2074
V7-3V	55	64	950	16	205	BD	2141
V10-1V	110	69	916	22	214	BD	2016
V10-2V	105	70	898	14	194	BD	2062
V7-10	61	62	948	15	189	BD	1924
TV930707-9	56	69	981	17	193	BD	1779
TV930709-1V	123	75	854	18	181	BD	1918
TV930709-2V	154	77	876	16	196	BD	1841
TV930705-2	92	69	913	19	198	BD	1756
Little Cottonwood stock							
072095-6	41	113	637	15	185	BD	1569
072095-8	55	122	589	8	180	BD	1922
072095-9	66	98	648	9	211	BD	1671
072095-11	57	121	648	8	200	BD	1533
072095-14	53	111	594	6	191	10	1454
072095-15	65	101	586	6	200	BD	1255
071895-4B	51	89	968	4	139	BD	1210
072095-16	46	125	543	7	161	12	1435
950720-LC-1	33	71	1047	14	177	BD	1156
950720-LC-2	44	115	635	15	163	11	1770
950720-LC-2A	52	109	559	15	191	12	1151
950720-LC-4	45	114	484	16	181	15	1165
950720-LC-5	60	104	590	12	193	BD	943
950720-LC-6	51	97	622	17	207	10	1433
950720-LC-7	39	108	589	12	179	7	1273
950720-LC-8	37	110	615	12	206	10	1220
Clayton Peak stock							
CP92-2	99	149	1060	33	327	BD	1819
CP92-3	86	196	815	28	406	BD	1500
CP92-4	89	200	760	26	388	12	1619
CP92-5	87	205	727	25	416	11	1818
CP92-6A	97	122	1005	23	353	BD	2136
CP92-6B	91	128	997	18	376	12	2111
TCP-2	85	208	731	25	419	14	1652
TCP-3	81	195	799	20	348	12	1828
C12-21	75	187	950	26	364	14	2199
C13-9	93	157	880	25	291	BD	2115
C13-12	90	130	919	21	338	BD	1751
C13-15	85	120	955	23	401	BD	2015
C13-18	88	180	844	26	441	13	2162
C14-1	80	129	964	24	317	BD	1956
C14-4	73	147	863	24	472	BD	1757
C14-12	63	118	879	18	357	16	1795
C15-3	81	95	916	24	340	BD	1808
C15-5	82	86	984	27	293	BD	2008
TC15-11	76	158	793	22	282	BD	1971
TCP-1	104	207	788	25	361	10	1838
93713-1	54	195	624	26	402	BD	1055
93713-14	80	123	934	25	355	BD	1421
93713-17	65	160	845	28	407	BD	1461
93715-13	87	98	785	17	257	BD	1051
TC93-15	73	125	912	30	431	BD	1558

Table 2 (Continued).

Sample	Zn	Rb	Sr	Y	Zr	Nb	Ba
Alta stock							
TALT-1	43	120	669	17	192	BD	1444
TALT-2	61	132	778	23	259	BD	1658
TALT-3	68	123	745	19	211	11	1293
TALT-4	71	68	951	22	128	BD	750
A92-1	56	104	783	20	205	BD	1510
A12-7	54	153	546	14	175	BD	1332
A12-11	49	126	733	15	211	BD	1494
A19-5	60	77	791	13	303	BD	1257
A19-8	60	98	729	10	223	BD	1447
A20-5	55	111	771	13	209	BD	1255
A20-10	54	106	677	15	213	BD	1408
A20-13	61	98	789	18	246	10	1665
A20-15	62	120	774	11	241	10	1473
A22-3	55	111	734	14	225	11	1274
A22-5	64	121	731	11	212	10	1615
93719-16	49	122	723	19	192	BD	1149
93719-17	32	105	651	17	188	BD	1011
93719-18	38	101	662	21	241	BD	1103
93719-23	61	129	709	24	215	BD	1141
93720-4	86	109	789	27	221	BD	1293
93720-9	45	122	588	17	203	BD	984
93720-11	38	111	739	16	206	BD	1187
93720-12	44	117	638	15	200	BD	1196
93722-8	56	97	707	18	220	BD	1060

Table 2 (Continued).

Sample	Zn	Rb	Sr	Y	Zr	Nb	Ba
Keetley volcanic rocks							
TK18-10	50	87	774	24	210	10	1730
15-5 I-80	76	114	978	24	362	BD	1955
15-9 I-80	75	70	966	20	251	BD	1799
15-11 I-80	55	94	803	23	340	BD	1823
15-14 I-80	76	58	849	22	234	BD	1994
15-15 I-80	64	69	990	25	262	BD	1937
20-14 I-80	76	78	937	26	252	BD	1907
20-17 I-80	68	66	898	22	228	BD	1744
20-18 I-80	55	68	843	19	225	BD	1641
20-19 I-80	72	71	959	20	261	BD	1779
20-3 FRAN	80	94	686	21	223	BD	1419
20-4 FRAN*	77	90	655	25	225	BD	1146
20-6 FRAN	80	90	700	26	239	BD	1223
20-11 FRAN	78	86	665	28	216	BD	1180
20-13 FRAN	78	97	777	24	249	BD	1295
18-12 PEO	75	163	789	26	529	14	1854
18-14 PEO	84	100	763	23	249	BD	1653
19-27 PEO	113	91	794	27	258	BD	1797
19-28 PEO	76	86	777	30	241	BD	1761
19-31 PEO	87	134	841	28	403	BD	2335
17-28 JD	77	122	896	26	273	BD	1414
18-8 JD*	101	73	952	38	333	BD	1497
18-9A JD	76	102	1007	34	310	BD	1628
18-9B JD	79	112	897	31	311	BD	1589
19-1 JD*	47	125	920	25	417	BD	1711
19-2 JD	90	45	987	29	266	BD	1555
19-3B JD	73	111	846	27	253	BD	1918
19-7 JD*	65	89	786	24	230	BD	1837
19-13 JD	76	92	903	26	239	BD	1829
19-16 JD	53	78	934	20	304	BD	1828
19-25 JD	99	111	856	34	312	BD	1460
19-32 JD	61	49	1099	27	234	BD	2285
19-33 JD	71	70	856	23	236	BD	1854
19-37 JD*	47	71	931	20	254	BD	1862
19-4 JD	65	55	827	18	222	BD	1701
19-9 JD	86	138	1402	24	553	BD	2607
19-10 JD*	74	138	1441	28	582	BD	2558
19-17 JD	71	87	933	28	267	BD	1565
Indian Hollow							
16-04 IH	71	90	830	21	220	BD	1429
16-09(*) IH	57	101	846	14	237	BD	1544
16-08 IH	69	107	894	24	254	BD	1433
16-10 IH	64	122	878	22	250	BD	1474
16-13 IH	73	117	1014	18	253	BD	1720
17-2 IH	68	127	830	18	251	BD	1476
17-13 IH	99	104	1165	32	378	BD	1607
17-23 IH	83	108	1426	24	285	BD	1968
17-24 IH	83	100	1410	25	278	BD	1935
17-25 IH	82	98	1401	30	280	BD	2085
17-31 IH	80	113	882	26	253	BD	1445

Table 3 (Continued on next page). ICP-MS and INAA analyses.

Sample	Sc	La	Ce	Sm	Eu	Tb	Yb	Lu	Hf	Th	Eu/Eu*
Little Cottonwood stock (ICP-MS)											
072095-8	2.29	49.7	92.1	4.61	1.09	0.34	0.44	0.06	4.33	9.51	0.91
072095-9	2.75	62.6	118.0	6.79	1.40	0.49	0.55	0.07	6.36	10.87	0.81
072095-16	4.53	30.4	67.9	5.09	1.15	0.44	0.94	0.14	4.82	12.41	0.83
950720-LC-4	4.71	58.6	109.2	5.80	1.19	0.55	1.60	0.25	8.09	17.06	0.73
950720-LC-6	4.38	44.2	89.6	5.68	1.34	0.49	0.94	0.14	5.52	8.79	0.87
950720-LC-8	4.08	45.8	90.8	5.32	1.23	0.42	0.77	0.11	5.30	7.33	0.87
Alta stock (ICP-MS)											
ALTA12-7	7.60	63.3	108.6	5.52	1.31	0.51	1.44	0.18	5.00	18.20	0.85
ALTA12-11	8.90	66.5	115.2	6.65	1.58	0.72	1.15	0.31	6.60	17.30	0.81
ALTA19-5	9.70	56.6	101.0	6.51	1.67	0.72	1.35	0.16	6.20	9.70	0.87
A22-3	7.09	61.8	113.6	6.96	1.63	0.61	1.53	0.23	5.13	12.68	0.85
93719-23	7.75	56.2	111.3	7.39	1.76	0.72	1.56	0.22	4.19	29.81	0.84
93722-8	8.35	42.9	89.6	6.08	1.51	0.53	1.43	0.21	3.98	9.58	0.91
93719-18	6.63	43.4	78.7	4.17	1.17	0.39	1.05	0.16	2.71	5.58	1.00
Clayton Peak stock (ICP-MS)											
TC12-21	16.30	95.5	183.0	11.60	2.37	1.01	1.74	0.25	10.10	31.80	0.75
TC13-9	13.50	88.4	167.8	9.60	2.17	0.87	1.40	0.20	9.70	28.00	0.81
TC13-12	17.80	83.2	158.4	10.10	2.39	1.01	2.03	0.25	11.00	21.40	0.83
TC15-5	22.30	71.9	138.5	9.90	2.43	0.88	1.63	0.26	7.20	12.70	0.89
TC15-11	10.10	86.1	156.4	8.40	1.82	0.70	1.01	0.11	7.90	22.00	0.80
Valeo stock (ICP-MS)											
TV93707-3V	8.40	72.6	128.6	6.89	1.65	0.60	0.92	0.14	5.50	9.80	0.87
To930718-9	8.45	56.3	103.2	6.38	1.50	0.62	1.61	0.24	4.90	17.58	0.83
TV-1	6.22	58.8	107.3	5.73	1.43	0.49	1.11	0.17	4.37	8.15	0.92
TV930707-9	8.77	34.0	65.2	4.91	1.32	0.49	1.28	0.19	4.21	5.21	0.94
TV930710-2V	7.54	33.9	65.5	4.84	1.34	0.50	1.26	0.18	4.46	4.99	0.96
TV930705-2	7.47	32.6	62.0	4.80	1.34	0.49	1.22	0.19	4.96	5.02	0.97
Mayflower stock (ICP-MS)											
TM93708-11	8.10	45.1	83.3	5.49	1.40	0.53	0.67	0.14	5.28	6.30	0.90
TM93710-5	10.90	66.7	116.2	6.86	1.68	0.71	1.81	0.19	6.56	14.70	0.84
TM93710-6	16.60	63.0	116.0	8.81	2.18	1.05	2.49	0.40	6.44	10.70	0.81
TM930710-11	10.16	52.3	96.9	6.09	1.51	0.62	1.72	0.25	5.21	11.04	0.86
TM930710-12	11.85	57.2	104.4	6.84	1.71	0.69	1.84	0.28	5.37	10.85	0.87

Table 3 (Continued).

Sample	Sc	La	Ce	Sm	Eu	Tb	Yb	Lu	Hf	Th	Eu/Eu*
Pine Creek stock (ICP-MS)											
TPC93705-10	9.50	61.3	105.5	7.07	1.67	0.67	1.41	0.18	5.79	8.10	0.84
TPC93705-12	10.10	70.8	130.2	7.18	1.74	0.63	1.29	0.16	6.50	9.60	0.88
P9-2	8.98	50.7	92.6	5.75	1.53	0.53	1.35	0.21	5.19	7.53	0.96
TPC93706-12	9.20	40.6	78.6	5.85	1.51	0.54	1.46	0.23	5.03	5.84	0.93
Ontario stock (ICP-MS)											
TO93711-5	8.60	67.4	114.8	6.56	1.65	0.57	1.21	0.15	5.50	18.20	0.92
TO93718-2	8.00	55.5	98.4	5.56	1.37	0.67	1.20	0.16	5.40	18.70	0.81
O11-3	8.38	53.4	97.3	5.78	1.43	0.59	1.65	0.25	5.32	17.92	0.86
O18-1	7.73	53.7	98.1	5.89	1.47	0.56	1.39	0.21	4.73	16.73	0.89
O18-3	8.68	58.6	107.1	6.42	1.56	0.62	1.53	0.22	5.55	17.42	0.86
Flagstaff Mountain stock (ICP-MS)											
TF93707-2	11.40	64.7	120.4	7.30	1.82	0.55	1.58	0.20	6.90	8.90	0.96
TF-3	10.47	49.4	93.2	6.31	1.62	0.62	1.62	0.25	5.73	7.17	0.90
F7-4	11.73	60.5	113.7	7.46	1.82	0.69	1.72	0.25	6.63	8.70	0.88
TF930703-4V	7.76	63.7	114.9	6.64	1.63	0.61	1.57	0.24	5.84	8.48	0.88
TF930707-7B	8.17	49.1	91.2	5.73	1.48	0.56	1.51	0.23	5.39	7.36	0.91
Keetley volcanic rocks (INAA)											
18-8 JD		95.6	166.6	11.73	2.82	1.18	2.91	0.47			0.84
19-1 JD		77.2	137.0	8.53	1.96	0.76	1.65	0.25			0.83
19-7 JD		59.2	100.7	5.91	1.63	0.57	1.56	0.21			0.97
19-10 JD		137.9	232.0	13.27	2.97	0.95	1.78	0.28			0.87
19-37 JD		68.7	128.6	6.29	1.73	0.55	1.49	0.23			1.00
20-4 Fran		55.8	101.6	6.82	1.69	0.70	2.09	0.33			0.86
TK 930718-6		63.9	110.7	6.39	1.88	0.59	1.49	0.26			1.05
TK 930718-9		87.2	155.3	9.12	2.25	0.85	2.05	0.30			0.88
TK 930718-14		68.2	122.9	7.25	1.94	0.79	2.09	0.33			0.91
Little Cottonwood stock (INAA)											
072095-15		69.0	140.4	6.39	1.51	0.48	0.68	0.10			0.99
080897-02		65.1	135.7	6.75	1.73	0.55	1.26	0.15			1.04
081297-01		41.0	85.1	3.78	0.98	0.38	1.25	0.20			0.98
081697-02		48.2	96.0	4.09	1.11	0.33	0.86	0.12			1.11
970807-05		69.3	134.8	5.89	1.45	0.49	1.06	0.22			0.99

mafic rocks) (Fig. 10), and this decrease is consistent with a small amount of apatite (and possibly sphene) fractionation. Apatite fractionation is required by the multiple linear regression modeling discussed below.

Age Relations

New K-Ar and $^{40}Ar/^{39}Ar$ data were presented by John et al. (1998) and Vogel et al. (1998). In addition, Vogel et al. (1998) presented new U-Pb, $^{40}Ar/^{39}Ar$, and fission-track data, and summarized the $^{40}Ar/^{39}Ar$, K-Ar, and fission-track data from the literature (Crittenden et al., 1973; Bromfield et al., 1977; Naeser et al., 1983; John et al., 1998). In light of the discussion by Vogel et al. (1998), we consider the zircon U-Pb method to yield the best estimates of emplacement ages because of the high closing temperature involved (>700 °C; Hodges, 1991). Using the zircon U-Pb data, the emplacement ages are: Little Cottonwood stock 30.5 ±0.5 Ma, Alta stock 34.3 ±1.5 Ma, Clayton Peak stock 35.5 ±1.5 Ma, and Ontario stock 36.0 ±2.0 Ma. The error bars overlap with all stocks except the Little Cottonwood stock. Biotite K-Ar and $^{40}Ar/^{39}Ar$ ages are consistent with the U-Pb ages (and with post-emplacement cooling/uplift) (Fig. 11). When all the data are considered, they indicate to us that the Little Cottonwood stock has the youngest emplacement age (~30.5 Ma), and that the other stocks and Keetley volcanic field were emplaced between 33.5–36.6 Ma (Fig. 11). Cross-cutting relationships can be used to indicate that the Clayton Peak stock is older than the Alta stock (John et al., 1998).

The oldest tephra in the basin-fill assemblage in the Tibble half-graben (Fig. 2) is 36.4 ±0.2 Ma (biotite $^{40}Ar/^{39}Ar$ plateau age). The lack of igneous components in strata beneath this tephra and the

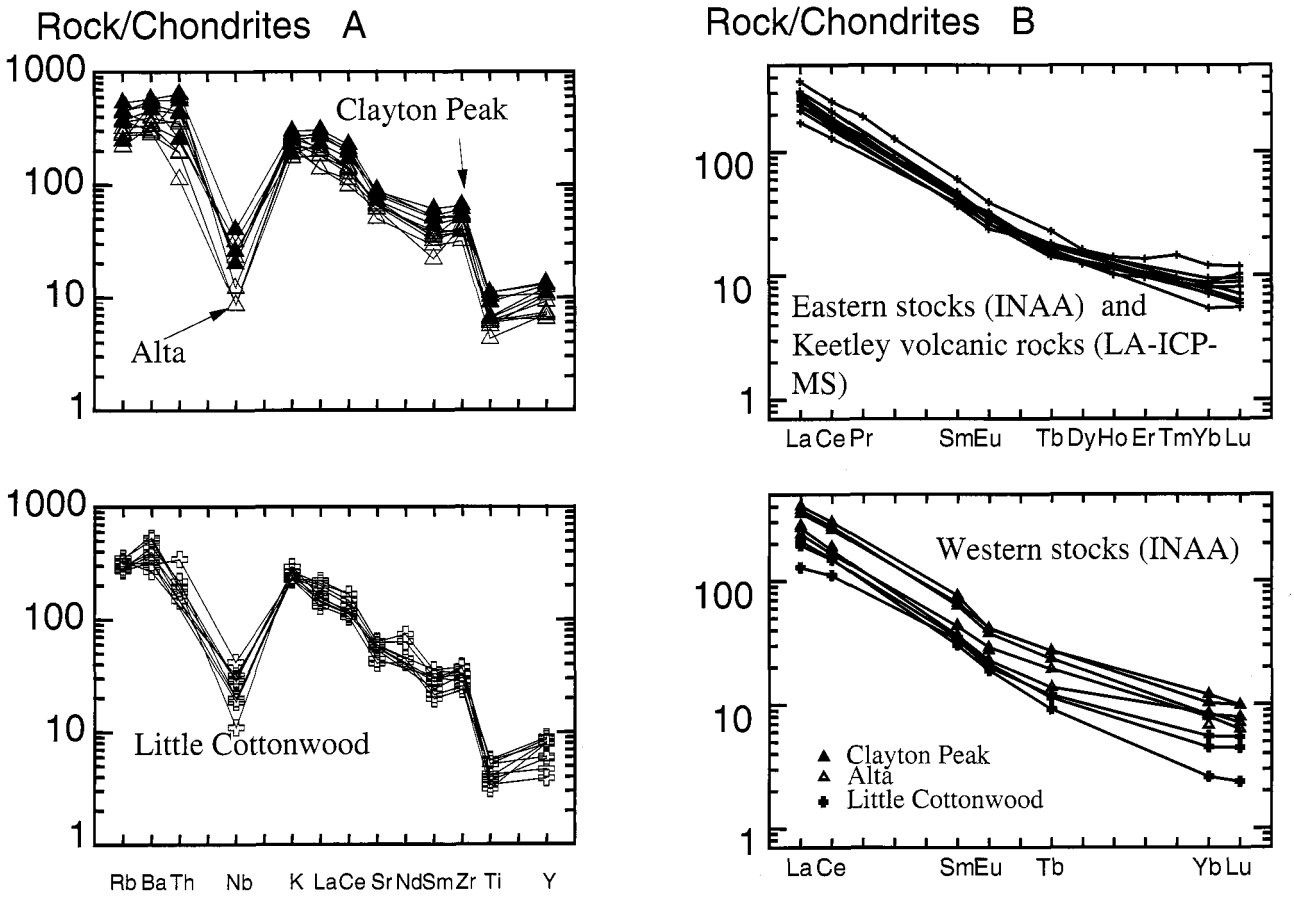

Figure 7. ***A,*** Chondrite-normalized (Sun and McDonough, 1989) spider diagrams for the western group of stocks (Little Cottonwood, Alta, and Clayton Peak stocks). The stocks from the eastern group are similar to the Alta stock. Note the large Nb anomaly that is typical of subduction-related rocks. ***B,*** Chondrite-normalized rare earth element diagrams for the eastern stocks and Keetley volcanic rocks (upper diagram) and western stocks (lower diagram). The data for the Keetley volcanic rocks are from LA-ICP-MS analyses at Michigan State University. All other data are INAA obtained at the Phoenix Laboratory, University of Michigan.

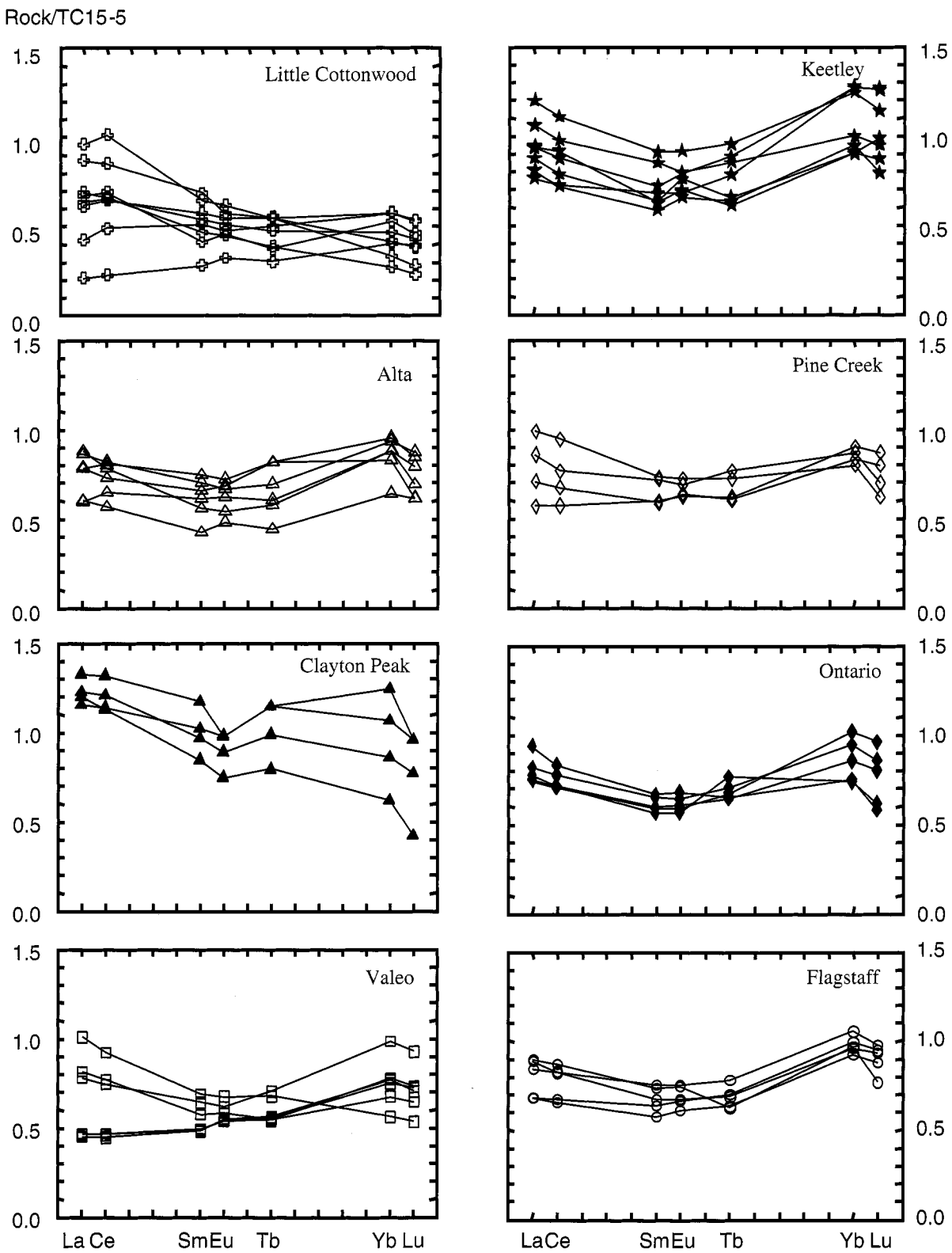

Figure 8. Rare earth element diagrams normalized to the most mafic sample from the Clayton Peak stock (TC15-5) for the stocks from the Wasatch igneous belt. The data for the Keetley volcanic rocks are LA-ICP-MS analyses at Michigan State University. All other data are INAA obtained at the Phoenix Laboratory, University of Michigan.

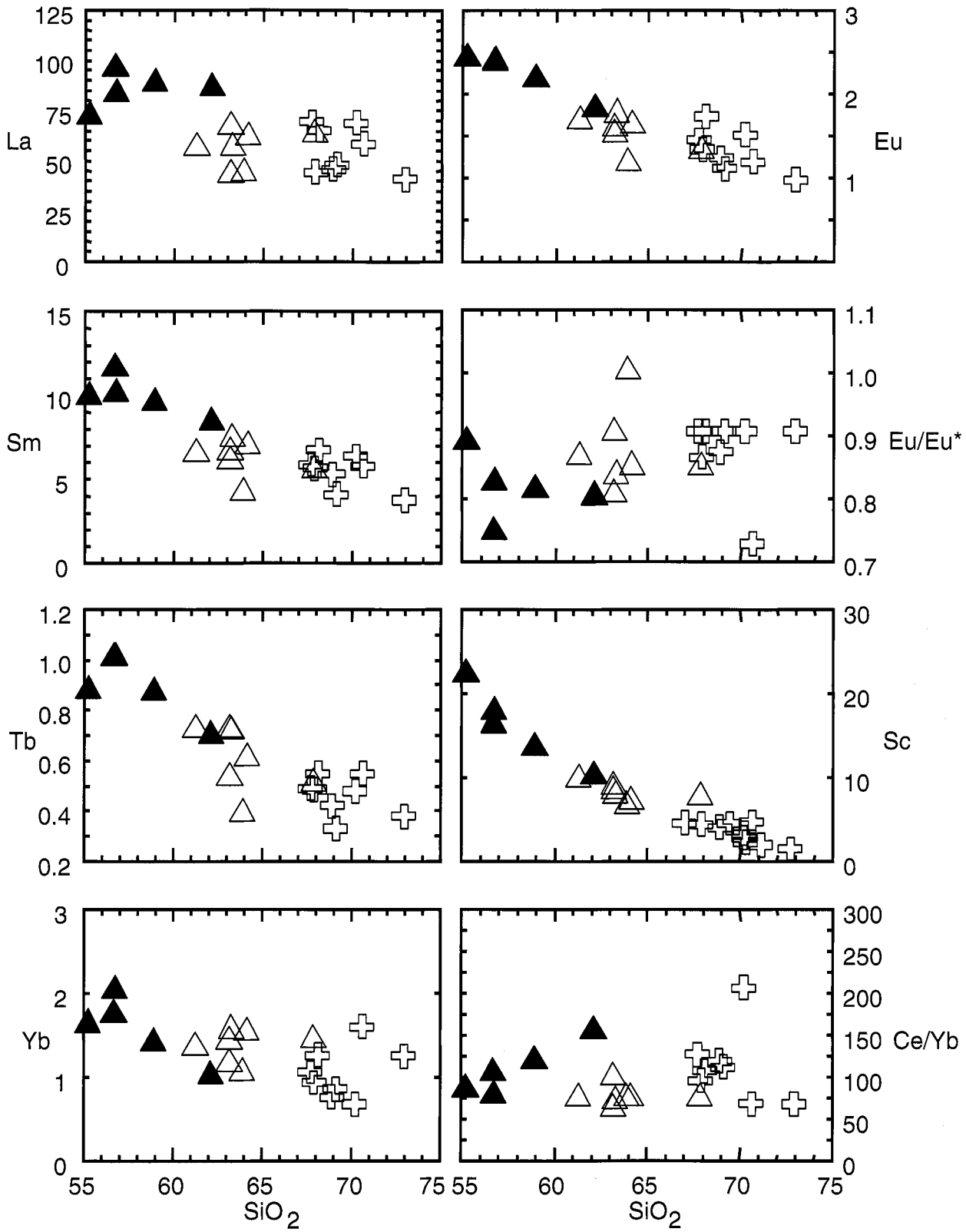

Figure 9. Variation of some trace elements and trace element ratios with silica content for the western stocks. Symbols are: open plus signs = Little Cottonwood stock, open triangles = Alta stock, filled triangles = Clayton Peak stock. There is a slight decrease in light and middle REEs (La, Sm, Eu, and Tb) with increasing silica content. There is no variation in the Eu anomaly (Eu/Eu*), which precludes a large amount of plagioclase fractionation. Ce/Yb is nearly constant with a large variation in silica content.

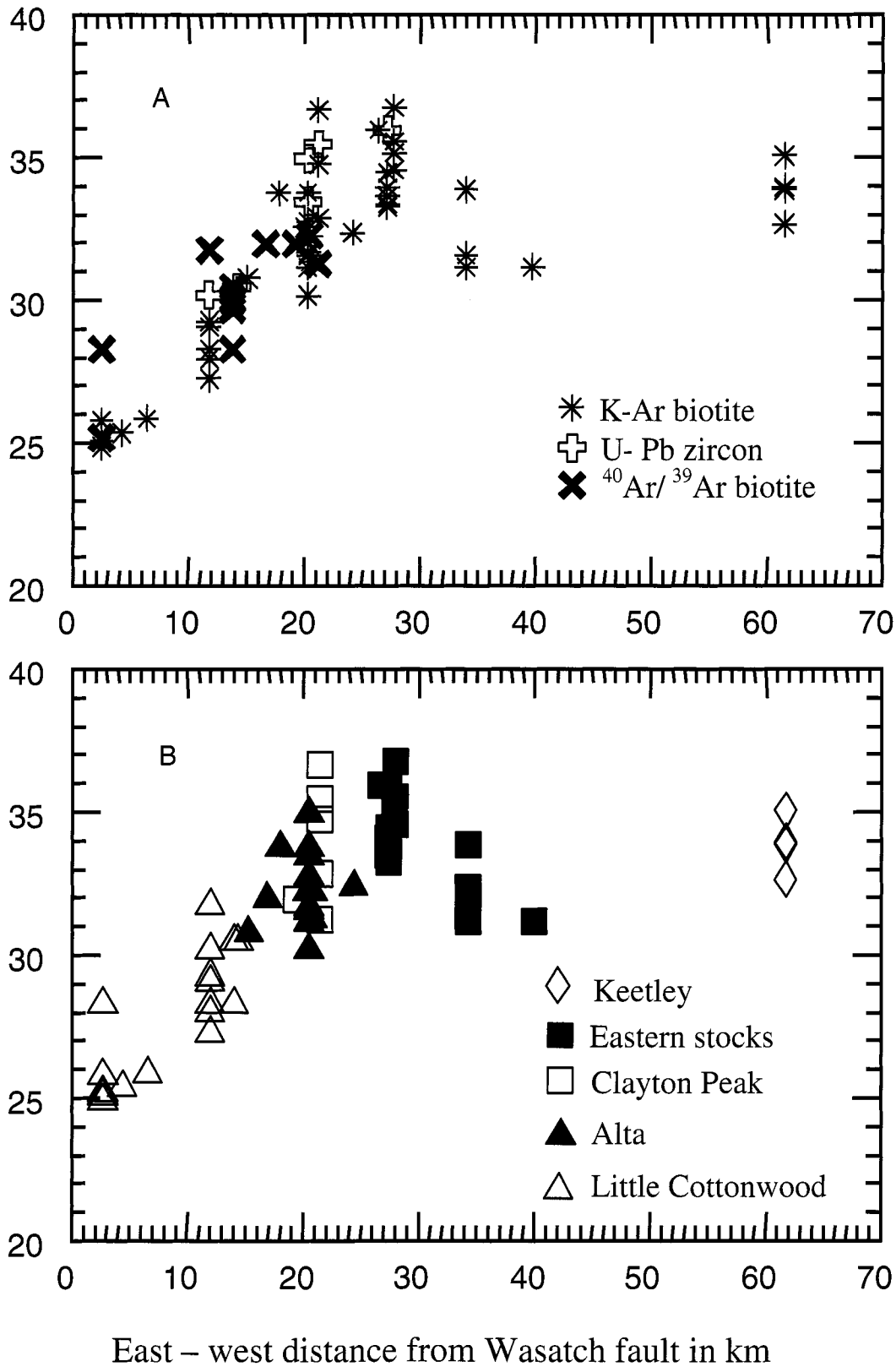

Figure 10. Age of the stocks in m. y. (vertical axis) versus relative horizontal distance from the Wasatch fault. U-Pb zircon reflects the highest closing temperatures and should reflect emplacement ages. The Little Cottonwood stock is younger than the other stocks as well as Keetley volcanic rocks (see text for discussion). Data are from Vogel et al. (1998), John et al. (1998), and Constenius (1998). ***A,*** Types of analyses; ***B,*** Names of stocks.

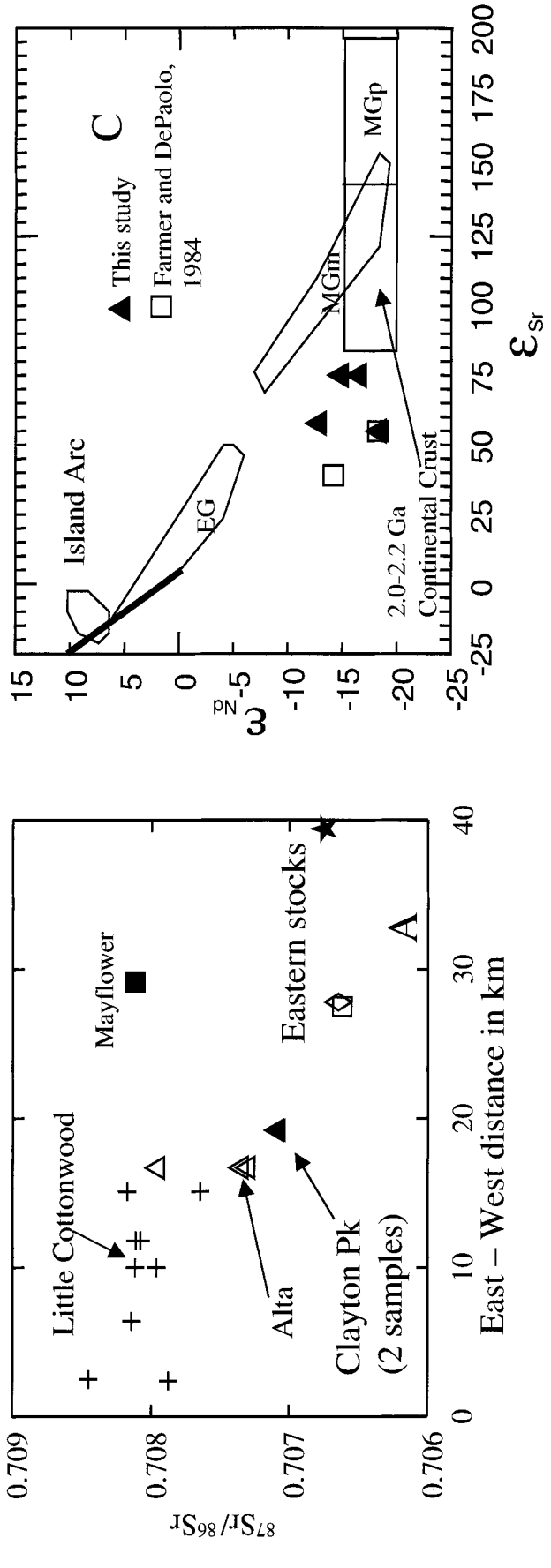

Figure 11. *A,* $^{87}Sr/^{86}Sr(i)$ for the stocks versus relative horizontal distance from the Wasatch fault (data from John, 1999, personal communication). There is a slight increase to the west with the Little Cottonwood stock containing distinctly higher $^{87}Sr/^{86}Sr(i)$ ratios. ***B,*** *f*(Sm/Nd) versus εNd(t) for the samples from the middle Cenozoic stocks compared to samples from the Archean [see text for discussion of *f*(Sm/Nd)]. Data from Carmela Garzione and Damian Hodkinson, University of Arizona). ***C,*** ε_{Nd} versus ε_{Sr}. Fields from Farmer and DePaolo (1984) are: eugeosycline and Sierra Nevada (EG); miogeosyncline peraluminous (MGp) and metaluminous (MGm) granites in Nevada. See Tables 4a and 4b.

close proximity of Tibble half-graben to the intrusive rocks and lavas of the central Wasatch Mountains support the idea that this tephra age may represent the maximum age for this igneous belt (Constenius et al., 1997; Constenius, 1998).

In using zircons for U-Pb dating, we tried to select pristine, unzoned grains that were devoid of inclusions. In spite of this, some of the zircons had inherited U-Pb ages. The inherited U-Pb ages, albeit a small sampling, fell into three groups: 2400–2200 Ma, ~1700 Ma, and 1050–900 Ma (Constenius, 1998, see his table 4-1). These age groupings are confirmed by a preliminary excimer laser U-Th-Pb study on zircons (J. M. Palin, personal comm., 2001). The provenance of these zircons likely corresponds to three crustal ages, which may represent the Archean-Paleoproterozoic Wyoming craton, Paleoproterozoic Yavapai province, and Uinta aulacogen, respectively. Obviously, much more work needs to be done on these inherited zircons. However, the three inherited-age groups of zircons are important in understanding the origin of these magmas.

Sr and Nd Isotopic Data

Sr and Nd isotopic data for the igneous rocks of the central Wasatch Mountains are given in Tables 4A and 4B. The $\varepsilon_{Nd(t)}$ are similar to most of the igneous rocks in the miogeocline (Farmer and DePaolo, 1983, 1984; Vogel et al., 1998, their fig. 9), but the $\varepsilon_{Sr(t)}$ are significantly lower (Fig. 11C). Farmer and DePaolo (1983, 1984) explained that this relationship is due to melting of a basement that had been previously depleted in Rb. One possible explanation for the dilemma of long-term depletion of Rb in rocks that have high potassium content is that the source rocks for the melts may have been recently enriched with Rb and K. Thus ^{87}Rb would not have been present to decay to ^{87}Sr. This recent enrichment in Rb may have occurred during the 100–40 Ma contractional deformation event, which was contemporaneous with dehydration of the subducting Farallon slab. This was followed by melting, perhaps of the Proterozoic crust (see below), during the middle Cenozoic (ca. 40–20 Ma) collapse of the thickened crust. If this were the case, the $\varepsilon_{Sr(t)}$ would be lower than expected based on the Rb content of the igneous rocks.

Crustal sources can be identified using the enrichment factor f_{Sm/Nd_t} versus $\varepsilon_{Nd(t)}$ (Fig. 11B and Table 4A), where

$$f_{Sm/Nd_t} = \frac{^{147}Sm/^{144}Nd_{sample}}{^{147}Sm/^{144}Nd_{UR}} - 1$$

and $^{147}Sm/^{144}Nd_{UR} = 0.1967$ (DePaolo and Wasserburg, 1976). The igneous rocks of the central Wasatch Mountains occur on a line intermediate between the 1650- and 1400-Ma depleted mantle lines. We interpret this to indicate derivation from partial melting of crustal rocks in that age range. On Figure 11B, it can be seen that the Archean Farmington Canyon complex and Archean of Idaho are much too enriched in Sr to have been the crustal end member.

There is a general increase in $^{87}Sr/^{86}Sr(i)$ from the east to the west (Fig. 11A). The Keetley volcanic field, eastern stocks, and Clayton Peak stock range from 0.7064 to 0.7069; the Alta stock has three analyses, two at 0.7071 and one at 0.7079. The $^{87}Sr/^{86}Sr(i)$ values for the Little Cottonwood stock range from 0.70736 to 0.70823 (D. A. John, personal comm., 2000). The Mayflower stock does not follow this trend, and the reason for this is unknown. The increase in $^{87}Sr/^{86}Sr(i)$ in the Alta and Little Cottonwood stocks to the west may indicate more interaction with high $^{87}Sr/^{86}Sr(i)$ rocks (Archean gneisses or Paleozoic carbonate rocks).

Discussion

Source of the Magmas

Even though there is a large range in major element concentrations (0.4–5.5 wt. % MgO; 1.9–7.7 wt. % Fe_2O_3), all of the igneous rocks from the central Wasatch Mountains have similar REE patterns (Figs. 8 and 9), and the relative variation in REE abundances is much less than the relative variation in major elements. Figure 8 shows the REEs normalized to the most mafic sample in the Clayton Peak stock (Tc 15-5). Figure 9 shows that there is little change in these trace element concentrations with silica concentration and that most of the samples show a decrease in REEs with increasing silica concentration. Most of the samples range from no depletion (with respect to the most mafic Clayton Peak sample) to 50% depletion (Fig. 8). Only a very few samples show enrichment in REE concentrations. The trace elements that are normally incompatible (REEs, Th, Sc, Hf, and Zr) decrease with increasing SiO_2 concentration in these rocks (Fig. 9). The relative abundance of these trace elements indicates that the concentration and the mineralogy of the source area, rather than fractional crystallization, were the controlling factors. We interpret the lack of any significant Eu anomaly to indicate that plagioclase was not present in the source rock unless large amounts of melting occurred. Plagioclase is unstable at depths above 10 kb (Springer and Seck, 1997).

Table 4a. Sr and Nd isotopic data (data collected by Carmela Garzione and Damian Hodkinson, Department of Geosciences, University of Arizona, Tucson, Arizona).

Unit Name	Sample No.	Nd	Sm	$^{87}Rb/^{86}Sr$	$(^{87}Sr/^{86}Sr)m$	$(^{87}Sr/^{86}Sr)i$	εSr	$^{147}Sm/^{144}Nd$	$(^{143}Nd/^{144}Nd)m$	εNd(m)	εNd(t)	T(DM)	f(Sm/Nd)
Clayton Peak stock	CP92-6	65.52	10.74	0.29390	0.70842	0.70827	54	0.09909	0.51185	-15.37	-14.93	1583	-0.50
Ontario stock	TO93711-3	36.62	5.77					0.09517	0.51184	-15.48	-14.96	1539	-0.52
Ontario stock	93718-2	35.34	5.50					0.09409	0.51183	-15.68	-15.16	1537	-0.52
Keetly volc.	K18-04	81.89	11.85	0.25538	0.70863	0.70850	57	0.08748	0.51167	-18.90	-18.41	1657	-0.56
Keetly volc.	K18-06	38.78	5.95	0.28969	0.70986	0.70971	75	0.09280	0.51180	-16.32	-15.86	1563	-0.53
Pine Creek	Tpc06-14	41.31	6.55	0.21693	0.70905	0.70894	64	0.09578	0.51176	-17.04	-16.59	1650	-0.51
Alta dike	Alt-D-29-4	57.50	9.39					0.09869	0.51196	-13.28	-12.86	1436	-0.50

Table 4b. Sr isotopic data from United States Geological Survey (David John, personal comm., 1999).

Sample No.	Unit	Rb	Sr	Rb/Sr	$^{87}Rb/^{86}Sr$	$^{87}Sr/^{86}Sr$	$^{87}Sr/^{86}Sri$	εSr
85-PC-1	Little Cottonw	105	588	0.17900	0.51700	0.70845	0.70823	53.39
85-PC-2	Little Cottonw	98	701	0.13994	0.40500	0.70808	0.70790	48.78
85-PC-3	Little Cottonw	99	704	0.14077	0.40700	0.70814	0.70797	49.70
85-PC-4	Little Cottonw	95	747	0.12731	0.36800	0.70811	0.70795	49.51
85-PC-5	Little Cottonw	108	614	0.17590	0.50900	0.70817	0.70795	49.51
85-PC-6	Little Cottonw	124	536	0.23134	0.66900	0.70765	0.70736	41.03
85-PC-7	Little Cottonw	169	445	0.37978	1.09900	0.70788	0.70740	41.67
83-PC-217	Little Cottonw	145	373	0.38874	1.12000	0.70812	0.70763	44.96
79-LC-112	Little Cottonw	122	536	0.22761	0.65800	0.70796	0.70768	45.61
82-PC-17	Alta	95	645	0.14744	0.42700	0.70730	0.70709	37.36
83-PC-206	Alta	123	701	0.17546	0.50800	0.70735	0.70710	37.51
83-PC-272	Alta	123	755	0.16291	0.47100	0.70795	0.70773	46.36
S-22	Clayton Peak	98	929	0.10527	0.30500	0.70709	0.70693	35.15
83-PC-167	Clayton Peak	139	889	0.15636	0.45200	0.70708	0.70685	33.94
81-PC-4	Valeo	66	906	0.07230	0.20900	0.70662	0.70650	29.04
81-PC-6	Pine Creek	62	838	0.07399	0.21400	0.70665	0.70652	29.40
82-PC-67	Mayflower	145	373	0.38874	1.12000	0.70812	0.70747	42.76
81-PC-8	Indian Hollow	111	1141	0.09728	0.28100	0.70675	0.70660	30.46

It is difficult to generate high-potassium, calc-alkaline rocks from mantle sources because the K_2O content of a mantle melt is too low to produce fractionation in the high-potassium field (Roberts and Clemens, 1993). In the case of the igneous rocks of the central Wasatch Mountains, the ε_{Sr} and ε_{Nd} data are not consistent with a direct origin from the mantle. Most important, as discussed above, in order to explain the low $\varepsilon_{Sr(t)}$ a long-term depletion of Rb is necessary. A possible explanation for these high-potassium rocks is that melting of the lower crust occurred as a consequence of extensionally driven decompression following Late Cretaceous to Eocene crustal thickening in the central Wasatch Mountains (Bryant and Nichols, 1988; Constenius, 1996, 1998, 1999). This deformation was due to the subduction of the Farallon plate. Dehydration of the slab during subduction of the Farallon plate may have produced Rb- and potassium-rich fluid, which metasomatized the lower part of the crust.

Our preferred model of magmatism in the Wasatch igneous belt involves partial melting of mafic to intermediate composition lower crust. This melting was due to two factors: 1) decompression resulting from collapse of the thickened crust that occurred simultaneously with, but disconnected from, northwest–southeast-oriented crustal extension, and 2) intrusion of mantle melts into the lower crust (Vogel et al., 1998). The extra heat provided by intrusion of mantle melts, combined with decompression, would cause relatively rapid crustal melting. These magmas most likely resulted from melting of Paleoproterozoic calc-alkaline crust, which then ascended along extensional accommodation zones in the crust. Important effects of this magmatism included thermal weakening of the crust and induced ductile behavior which, in turn, led to inflation of the magma chambers (Lister and Baldwin, 1993).

Decompression melting was driven by both collapse of the crustal welt and left-lateral shearing parallel with the Paleoproterozoic-Archean boundary. This shearing would have allowed mantle upwelling and underplating of the lower crust by mafic magmas, further aiding melting of the hot lower crust (Paleoproterozoic metaigneous rocks) and resulting in formation of high-potassium, calc-alkaline magmas with the ε_{Nd} and ε_{Sr} values that we observe for these rocks.

Because of the absence of Eu anomalies in the igneous rocks, decompression melting most likely occurred at pressures where plagioclase was not stable. Rocks from these depths are not exposed at the surface. However, assuming that the surface rocks were once at these depths, we did reconnaissance chemical analyses (Table 5) on the Precambrian rocks exposed in the area. They include the Farmington Canyon complex (Archean), Little Willow Formation (Paleoproterozoic?) (Bryant, 1992), and the Santaquin complex (Paleoproterozoic) (S. Nelsen, personal comm., 2001). Our purpose was to determine if these could have been source rocks for the igneous rocks of the central Wasatch Mountains. The Farmington Canyon complex consists of high-grade gneisses, schists, and migmatite with abundant pegmatite (Bryant, 1988, 1992). The Little Willow Formation consists of lower grade schists, gneisses, and migmatite with concordant layers and lenses of amphibolite up to 100 meters in thickness (Kohlmann, 1980; Bryant, 1988, 1992). The Santaquin complex consists of gneiss, schist, and amphibolite as well as intrusions of granite and minor pegmatite (Eardley, 1933; Demars, 1956).

The REE distributions for samples of the Farmington Canyon complex, Santaquin complex and amphibolitic (mafic) rocks from the Little Willow Formation are shown in Figure 12. Only samples that exhibit relatively flat distribution of REE patterns can represent possible source rocks for the igneous rocks of the central Wasatch Mountains. The $^{87}Sr/^{86}Sr_i$ and $f_{(Sm/Nd)t}$ (Hedge et al., 1983) of the Farmingon Canyon complex (Fig. 11) are much too high to represent a reasonable source for magmas. Furthermore, ε_{Nd} values of the Farmington Canyon complex are too low (ε_{Nd} of $\sim$30) to allow its consideration as the major source for the magmas. Considering the REE-distribution patterns, the mafic rocks from the Little Willow Formation are potential source rocks. However, no Sr or Nd isotopic studies have been done on these rocks.

Modeling of batch melting of a mafic source such as the amphibolites in the Little Willow Formation demonstrates that 10–15% melting of a source that contains clinopyroxene and garnet can duplicate the REE abundances of the igneous rocks from the central Wasatch Mountains (Fig. 13A). Most of the other incompatible trace elements can be similarly modeled. On a spider diagram (Fig. 13B), except for Nb, all elements are consistent with 10–15 % melting of a rock with similar composition to the mafic portion of the Little Willow Formation at a depth below the stability of plagioclase (eclogite-facies metamorphic conditions). If some ilmenite is included in the source, the Nb concentration is also consistent with this model.

Table 5a (Continued on next page). Major element analyses of Precambrian rocks that occur in the area.

XRF analyses

Sample	SiO_2	TiO_2	Al_2O_3	Fe_2O_3	MnO	MgO	CaO	Na_2O	K_2O	P_2O_5
Proterozoic: Santaquin complex										
051798-10	44.48	1.17	7.86	16.47	0.26	10.03	17.40	0.80	0.62	0.16
051798-12	68.79	0.28	14.54	2.56	0.04	0.26	0.78	2.41	7.93	0.06
051798-18	60.58	1.08	16.09	8.03	0.12	3.57	2.52	4.02	2.52	0.26
051798-1A	51.93	0.70	12.07	11.18	0.24	10.74	9.22	2.48	0.76	0.16
051798-4	72.52	0.26	14.06	2.25	0.03	0.33	0.29	2.85	6.79	0.06
051798-7A	56.03	0.62	17.92	7.24	0.14	4.16	6.36	4.36	2.02	0.19
Proterozoic: Little Willow Formation - amphibolites										
KNC 10698-1	52.77	0.72	14.42	12.18	0.20	6.95	9.12	2.61	0.79	0.06
KNC 10698-5	51.74	0.69	14.38	11.83	0.21	8.03	8.11	2.96	1.07	0.06
KNC 10698-6	51.23	0.67	14.45	11.52	0.20	8.31	8.63	3.20	0.85	0.05
KNC 10698-7	52.61	0.72	12.40	12.21	0.22	9.19	8.73	2.08	1.17	0.06
KNC 10698-8	53.12	0.70	13.88	11.69	0.24	7.44	7.97	3.28	0.73	0.06
Archean: Farmington Canyon complex										
62098-11	67.53	1.02	12.73	9.66	0.23	0.66	2.73	1.78	2.48	0.29
62098-13	64.55	0.20	19.33	2.72	0.03	1.08	0.56	9.60	0.12	0.22
62098-2	76.91	0.57	11.35	5.25	0.11	1.64	1.76	1.90	1.71	0.09
62098-4	57.67	0.77	13.43	9.79	0.16	5.41	9.03	0.49	1.04	0.07
62098-6	50.54	0.77	17.72	10.42	0.15	5.94	10.37	0.67	2.26	0.05

XRF analyses

Sample	Cr	Ni	Cu	Zn	Rb	Sr	Y	Zr	Nb	Ba
Proterozoic: Santaquin complex										
051798-10	137	57	29	112	20	586	25	108	BD	295
051798-12	BD	BD	BD	55	226	106	51	275	14	986
051798-18	BD	14	BD	86	75	129	21	214	10	629
051798-1A	649	144	19	87	21	305	15	70	BD	155
051798-4	BD	BD	BD	34	238	55	22	175	13	515
051798-7A	77	60	11	86	59	762	11	92	BD	709

Table 5a (Continued).

XRF analyses

Sample	Cr	Ni	Cu	Zn	Rb	Sr	Y	Zr	Nb	Ba
Proterozoic: Little Willow Formation - amphibolites										
KNC 10698-1	BD	92	181	101	24	173	15	58	5	141
KNC 10698-5	12	107	116	967	36	127	13	56	5	232
KNC 10698-6	18	116	74	81	29	170	15	52	6	156
KNC 10698-7	23	119	21	108	40	125	14	56	6	171
KNC 10698-8	84	102	81	135	24	177	14	57	6	138
Archean: Farmington Canyon complex										
62098-11	BD	23	11	159	126	30	149	804	43	1007
62098-13	BD	BD	BD	7	BD	7	41	135	16	BD
62098-2	13	44	186	79	84	114	49	259	14	554
62098-4	34	55	85	79	57	251	20	94	7	182
62098-6	27	60	33	84	127	240	16	51	5	225

Table 5b. Rare earth element analyses of Precambrian rocks that occur in the area.

ICP-MS analyses

Sample	La	Ce	Nd	Sm	Eu	Tb	Dy	Ho	Er	Tm	Yb	Lu
Proterozoic: Santaquin complex												
051798-10	31.37	73.62	53.75	11.95	2.89	1.28	6.33	1.17	3.06	0.39	2.34	0.32
051798-12	113.43	267.53	83.44	13.49	1.75	1.54	7.67	1.47	4.09	0.57	3.00	0.47
051798-18	26.68	50.77	22.35	4.55	1.31	0.71	3.65	0.71	2.06	0.32	1.82	0.29
051798-1A	13.99	30.28	16.64	3.92	1.05	0.56	3.39	0.66	2.02	0.29	1.80	0.27
051798-4	64.64	156.02	41.75	6.42	0.83	0.45	2.09	0.41	1.17	0.19	1.50	0.17
051798-7A	33.11	62.99	29.03	4.97	1.35	0.45	2.18	0.37	1.08	0.16	0.92	0.14
Proterozoic: Little Willow Formation - amphibolites												
KNC 10698-1	7.29	15.01	8.47	2.46	0.87	0.42	2.83	0.52	1.54	0.24	1.43	0.21
KNC 10698-5	6.46	14.13	7.56	2.22	0.74	0.43	2.53	0.52	1.46	0.24	1.69	0.21
KNC 10698-6	5.49	11.84	6.28	1.74	0.71	0.34	2.43	0.42	1.32	0.20	1.20	0.20
KNC 10698-7	5.84	13.27	8.05	2.37	0.76	0.44	2.85	0.50	1.44	0.24	1.56	0.21
KNC 10698-8	5.34	11.63	6.62	2.30	0.74	0.47	2.64	0.52	1.56	0.23	1.53	0.25
Archean: Farmington Canyon complex												
62098-11	46.60	81.96	41.15	8.55	1.10	1.54	9.25	2.07	6.77	1.04	6.75	1.10
62098-13	2.59	8.23	5.02	1.54	0.41	0.34	1.77	0.37	1.19	0.16	1.11	0.14
62098-2	37.68	72.23	30.73	5.96	1.34	1.04	6.30	1.58	5.27	0.87	5.64	0.83
62098-4	15.24	29.88	14.17	3.33	0.92	0.56	3.50	0.72	2.32	0.33	2.10	0.33
62098-6	5.15	10.88	6.72	1.71	0.68	0.37	2.32	0.51	1.56	0.21	1.50	0.23

Origin of the Chemical Diversity

There is a large variation in major element compositions in the igneous rocks from the central Wasatch Mountains, and this variation occurs in three distinct compositional groups. Samples of the Clayton Peak stock are in the most mafic group. Samples of the Alta stock, eastern stocks, and Keetley volcanic rocks occur in a second group of intermediate composition. Samples of the Little Cottonwood stock are in a third group, the most silicic of the three. Fractional crystallization can produce the variation in major element concentrations observed within each of the groups. However, age and isotopic differences among the three chemical groups preclude differentiation from a single magma as an explanation for the three compositional groups of magmas. Based on field relationships and U-Pb zircon ages, we interpret the Clayton Peak stock as one of the earliest plutons. The compositional variation within the Clayton Peak stock is consistent with crystal fractionation dominated by clinopyroxene, orthopyroxene, and plagioclase with minor separation of ilmenite and magnetite (Table 6). The entire variation within the stock can be modeled by multiple linear regression (Bryan, et al., 1969; Wright and Dougherty, 1970) in two steps with the sum of the squares of the residuals being 0.015 and 0.206, respectively. Similarly, the compositional variation within the Alta stock (intermediate-composition group) can be modeled in two steps by separation of the same phases (with the addition of apatite as a fractionating phase) (Table 6) with the sum of the squares of the residuals of 0.017 and 0.088, respectively. The compositional variation of the Little Cottonwood stock can also be modeled in two steps. However, in this case pyroxenes are not required as fractionating phases whereas K-feldspar is required (Table 6). The sum of the squares of the residuals is 0.067 and 0.040, respectively. Because the compositional variation in the eastern stocks and Keetley volcanic rocks is similar to that of the Alta stock (intermediate-composition group), the overall pattern of major element compositional variation within this group can be produced by crystal fractionation. This large compositional variation in volcanic rocks compared to the stocks may be due to the fact that volcanic rocks may be a sample of a wide variety of magma bodies, whereas each stock represents one magma body that crystallized as a coherent body (which may have formed by coalescence of different magma batches). The compositional variation among the three groups reflects magmas generated from a common source that have evolved primarily by crystal

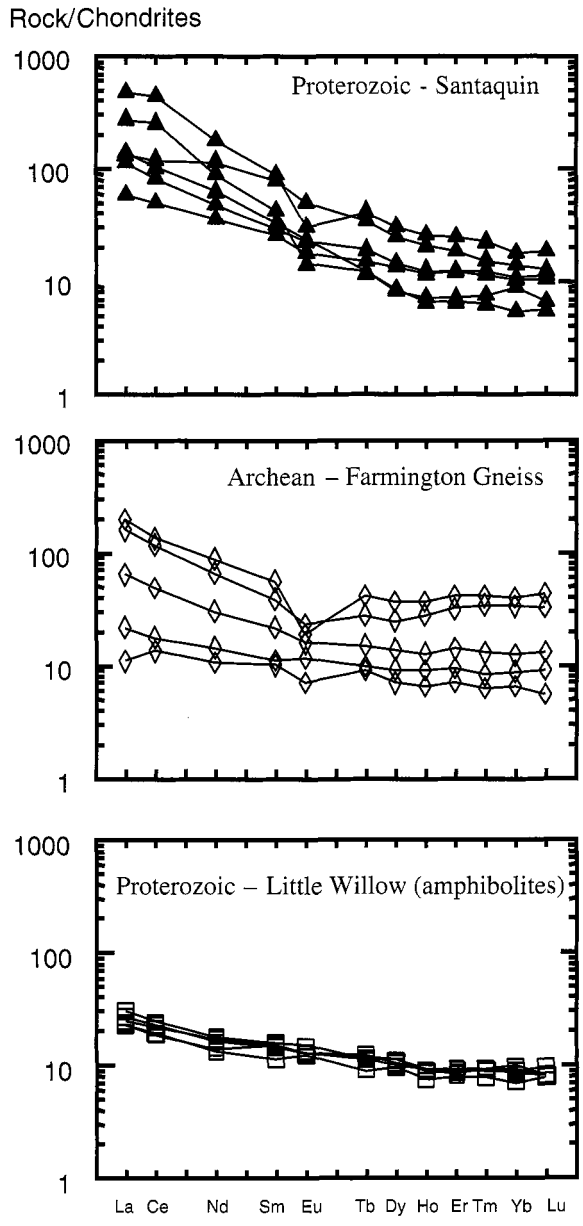

Figure 12. Chondrite-normalized REE distribution (Sun and McDonough, 1989) for the Proterozoic Santaquin and Little Willow Formations and Archean Farmington Gneiss. Only the mafic rocks (amphibolites) from the Little Willow Formation are possible source-rock compositions for magmas of the Wasatch igneous belt.

fractionation, and most likely magma recharge, from at least three separate magma bodies. The Clayton Peak magma is the oldest, least evolved and least affected by crustal contamination. The Little Cottonwood magma is the youngest, most evolved, and the most affected by crustal contamination.

Although there is very little variation in REE abundance in the igneous rocks of the central

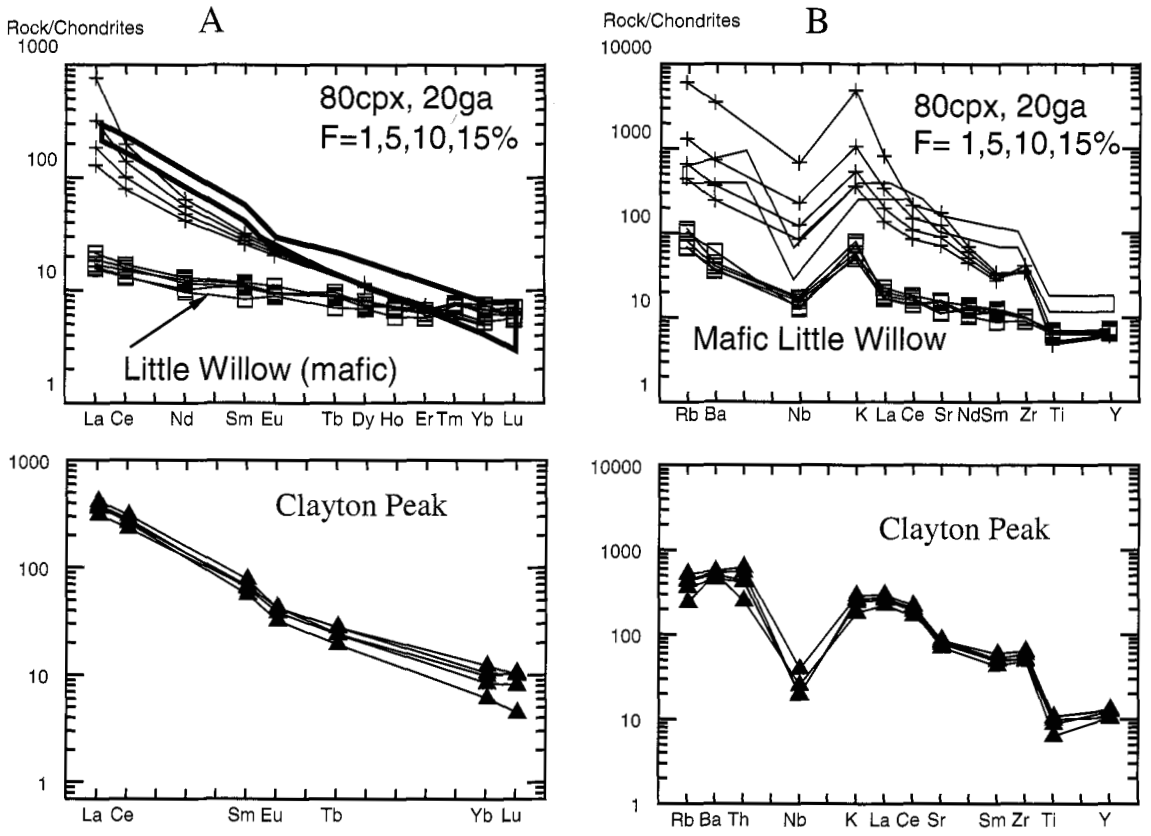

Figure 13. ***A,*** REE-modeling diagram showing that partial melting of 10–15% of the mafic rocks (amphibolite) from the Little Willow Formation can produce the composition of the Clayton Peak stock. Model assumes an eclogite source with 80% clinopyroxene and 20% garnet (distribution coefficients from Patino, 1997). ***B,*** Incompatible-element spider diagram showing that partial melting of 10–15 % of mafic rocks (amphibolite) from Little Willow Formation can, except for Nb, produce the composition of the Clayton Peak stock. Model assumes an eclogite source with 80% clinopyroxene and 20% garnet. If a small percentage of ilmenite is included, the Nb abundance is consistent with the composition of the Alta stock.

Wasatch Mountains, closer inspection demonstrates a slight, systematic decrease in the REEs with increasing silica content (except for the most mafic rocks), and this decrease is especially notable with the middle REEs (Sm, Eu, and Tb) (Fig. 8). This variation is consistent with a small amount of apatite (and possibly sphene) fractionation, which is required by the major element linear regression modeling. There is no systematic Eu/Eu* variation with silica content (Fig. 9), and this lack of a Eu anomaly precludes any large amount of plagioclase fractionation with increasing silica content in these rocks. The calculated REE concentrations using the minerals from the multiple linear regression (Table 6) calculations are consistent with the actual REE distributions.

PART II. ASCENT AND EMPLACEMENT OF COMPONENTS OF THE WASATCH IGNEOUS BELT

Structural Setting

Late Cretaceous to middle Cenozoic magmatism and deformation in the Cordillera of the southwestern United States and Mexico have been attributed to subduction of a low-angle slab and subsequent rollback (Coney and Reynolds, 1977). The former process is associated with crustal shortening and the latter one with crustal extension, driven in part by gravitational collapse of the orogen (Coney and Reynolds, 1977; Engebretson et al., 1985; Dickinson, 1991; Wernicke, 1992; Ward, 1995; Sterne and

Table 6. Fractional crystallization models.

Clayton Peak Stock Step I

Fractionating Phases	Amount in %
Clinopyroxene	5.4
Orthopyroxene	5.5
Plagioclase (An47)	13.1
Magnetite	0.5
Ilmenite	0.6

Parent = TC15-5
Daughter = TC13-12
Liquid remaining 75.0%
Sum of the squares of the residuals 0.015

Clayton Peak Stock Step II

Fractionating Phases	Amount in %
Clinopyroxene	6.1
Orthopyroxene	1.6
Plagioclase (An47)	4.9
Magnetite	0.3
Ilmenite	0.4

Parent = TC13-12
Daughter = TC13-9
Liquid remaining 86.0%
Sum of the squares of the residuals 0.206

Clayton Peak Stock Step III

Fractionating Phases	Amount in %
Clinopyroxene	3.8
Orthopyroxene	2.6
Plagioclase (An47)	10.8
Magnetite	0.6
Ilmenite	0.7

Parent = TC13-9
Daughter = TC15-11
Liquid remaining 80.2%
Sum of the squares of the residuals 0.574

Alta Stock Step I

Fractionating Phases	Amount in %
Clinopyroxene	3.4
Orthopyroxene	1.9
Plagioclase (An47)	11
Magnetite	0.5
Ilmenite	0.3
Apatite	0.3

Parent = Alta19-5
Daughter = 93719-18
Liquid remaining 82.8%
Sum of the squares of the residuals 0.017

Alta Stock Step II

Fractionating Phases	Amount in %
Clinopyroxene	4.2
Orthopyroxene	0.0
Plagioclase (An47)	21.2
Magnetite	01.7
Ilmenite	0.5
Apatite	0.0001

Parent = 93719-18
Daughter = Alta12-7
Liquid remaining 72.0%
Sum of the squares of the residuals 0.088

Little Cottonwood Stock Step I

Fractionating Phases	Amount in %
Plagioclase (An29)	2.6
Magnetite	0.4
Ilmenite	0.2
Apatite	0.3

Parent = 950720-LC6
Daughter = 072095-16
Liquid remaining 96.2%
Sum of the squares of the residuals 0.067

Little Cottonwood Stock Step II

Fractionating Phases	Amount in %
Plagioclase (An29)	2.7
K-feldspar	4.8
Magnetite	0.3
Ilmenite	0.0
Apatite	0.1

Parent = 072095-16
Daughter = 950720-LC4
Liquid remaining 91.7%
Sum of the squares of the residuals 0.040

Constenius, 1997). Constenius (1996, 1998) has proposed a similar sequence in the Wasatch region of Utah. The crustal shortening that produced the Cordilleran fold-and-thrust belt was followed by gravitational collapse, which began in early middle Eocene (ca. 49–48 Ma) and terminated in early Miocene (ca. 20 Ma). The collapse took place on low-angle detachment surfaces that originated as thrusts during the earlier contractional phase. Crustal collapse was accompanied by the development of metamorphic core complexes and regional magmatism. In particular, Constenius (1998) states that the ascent and emplacement of the igneous rocks of the central Wasatch Mountains can be attributed to decompression melting as a result of the unroofing of the Little Cottonwood core complex by a detachment fault that initiated along the pre-existing Charleston-Nebo thrust. The earlier contractional deformation transported the Charleston-Nebo thrust sheet to the east, and it now forms a U-shape, opening to the west (Fig. 2). During the contractional phase the northern, east–west-trending trace of the thrust that now parallels the middle Cenozoic stocks was a lateral ramp with a component of left-lateral slip. At the time of collapse, the sense of motion was a right-lateral fault (Paulsen and Marshak, 1998). Constenius (1998) reports kinematic indicators giving a west-southwest sense-of-shear for the hanging wall, consistent with right-lateral slip during collapse. However, the stress pattern inferred from the dikes indicates northwest-southeast extension (Cambray and Holst, 1993; Vogel et al. 1998). If as we propose strike-slip motion was involved, it must have been left lateral. East-west linear belts have been shown to be the loci of much of the Cenozoic igneous activity in the western United States (Rowley, 1998). In this part of the paper, we present a model that explains the east-west alignment of the igneous rocks in the central Wasatch Mountains as being associated with deep-seated strike-slip motion, resulting from continued convergence at depth. This strike-slip displacement implies that convergence was still occurring concurrent with extension related to gravitational collapse in the supracrustal thrust sheets. A similar tectonic pattern has been described in the present-day Himalayas (England and Houseman, 1988; Burchfiel et al., 1992). Details of the geology of the region adjacent to the plutons are provided by John (1989a). Shortening features related to the Sevier orogenic belt and subsequent collapse are discussed by Constenius (1996).

In the first part of the paper, we demonstrated that the magmas were generated from a common source and rose to varying levels in the crust along an east-west linear zone that lies above a Paleoproterozoic suture. They rose through the Precambrian crust into the overlying deformed Proterozoic and Paleozoic strata. Uplift associated with the Wasatch fault produced a regional tilt to the east (John, 1989a) that now provides a cross section exposing the youngest and most deeply emplaced stock, the Little Cottonwood stock at the western end of the belt, whereas preserving the associated volcanic rocks at the eastern end. We focus on the Little Cottonwood stock in this part of the paper. The model presented for the ascent and emplacement relates the linear belt to an irregular zone of left-lateral strike-slip motion with very little displacement. Sidewall normal faults developed at stepovers (Fig. 14) in the manner described by Dooley and McClay (1997), and gave rise to pull-apart structures at the surface (Fig. 15). At depth, ramps on the normal fault gave rise to an extensional duplex (Gibbs, 1984) that became the site where the magma was arrested (Fig. 16). Additional space was created by collapse of the rock beneath the intrusion into the space vacated by the magma in the manner described by Cruden (1998) and McNulty et al. (2000).

The Problem of Ascent and Emplacement

The ascent of magmas from the site of initial melting to the final location of crystallization has been explained by combinations of diapiric rise and fracture-permitted movement (Hutton, 1988); i.e., the forceful versus passive emplacement models. This debate continues, and the question remains unresolved because the dynamic and thermal effects associated with intrusions tend to destroy much of the evidence needed to make a clear-cut case. Only partial evidence of each step remains and later events overprint earlier ones. With diapiric rise it is hard to explain the continued ability of the magma to flow through a progressively cooling crust that becomes more rigid at higher levels. With respect to passive explanations, Paterson and Schmidt (1999) have noted the difficulty in making a clear connection between fractures or faults and the path of the magma. Paterson and Fowler (1993) have drawn a useful distinction between creating space in the immediate vicinity of the pluton (i.e., near-field transfer processes), as opposed to large-scale translations of the crust (i.e., far-field transfer processes). Near-field transfer processes include evidence of deformation in the aureole. Several processes can be associated with far-field

material transfer processes: 1) large-scale stoping whereby pre-pluton rock exchanged places with the magma; 2) downward movement of the Moho or upward movement of the Earth's surface; and 3) creation of space by horizontal extension and transfer of the extra volume to a consuming plate margin (mid-ocean ridge magmatism is an example of this interrelationship). These processes, ably discussed by Hutton (1988) and Paterson and Fowler (1993), are difficult to demonstrate in any one locality. Our evidence for the ascent and emplacement of the Little Cottonwood stock suffers from the same dilemma discussed above; the evidence is not complete. Our model envisions dike-assisted ascent into space created by a combination of local extension in an extensional duplex associated with strike-slip faulting, stoping, and collapse of material below the pluton.

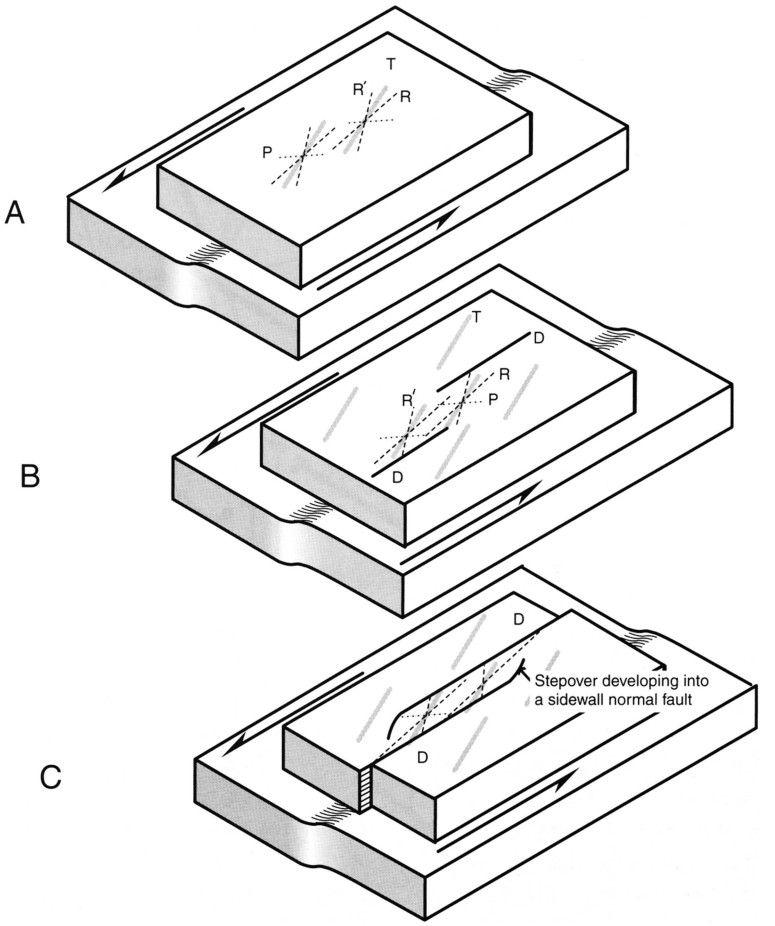

Figure 14. ***A,*** Development of Riedel shears (R and R'), tension fractures (T), and thrust shears (P) in the upper brittle crust above a left-lateral ductile shear zone in the lower crust. ***B,*** Development of displacement shears connecting R and T shears. ***C,*** Stepovers forming sidewall normal faults.

Significance of the Dikes

As we discussed in Part 1, the region is characterized by a set of dikes similar in age and chemistry to the stocks. The stocks crosscut some dikes but are themselves intruded by other dikes. The measured orientation of 166 dikes shows a strong northeast-southwest strike (Cambray and Holst, 1993; Vogel et al., 1998) (Fig. 17). The dikes are restricted to a belt closely associated with the stocks and volcanic rocks. We interpret the orientation of these dikes as a result of a stress field concurrent with the emplacement of the plutons with σ_1 trending northeast-southwest and σ_3 trending northwest-southeast. The association of the dikes with a linear belt and the lack of any regional features suggesting a similar stress pattern at this time

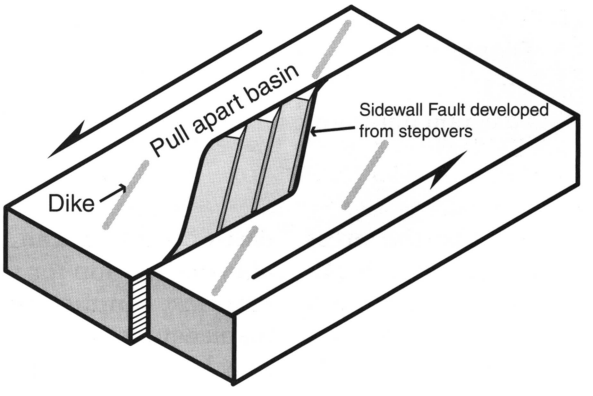

Figure 15. A long pull-apart basin developed with little offset between two widely spaced stepovers.

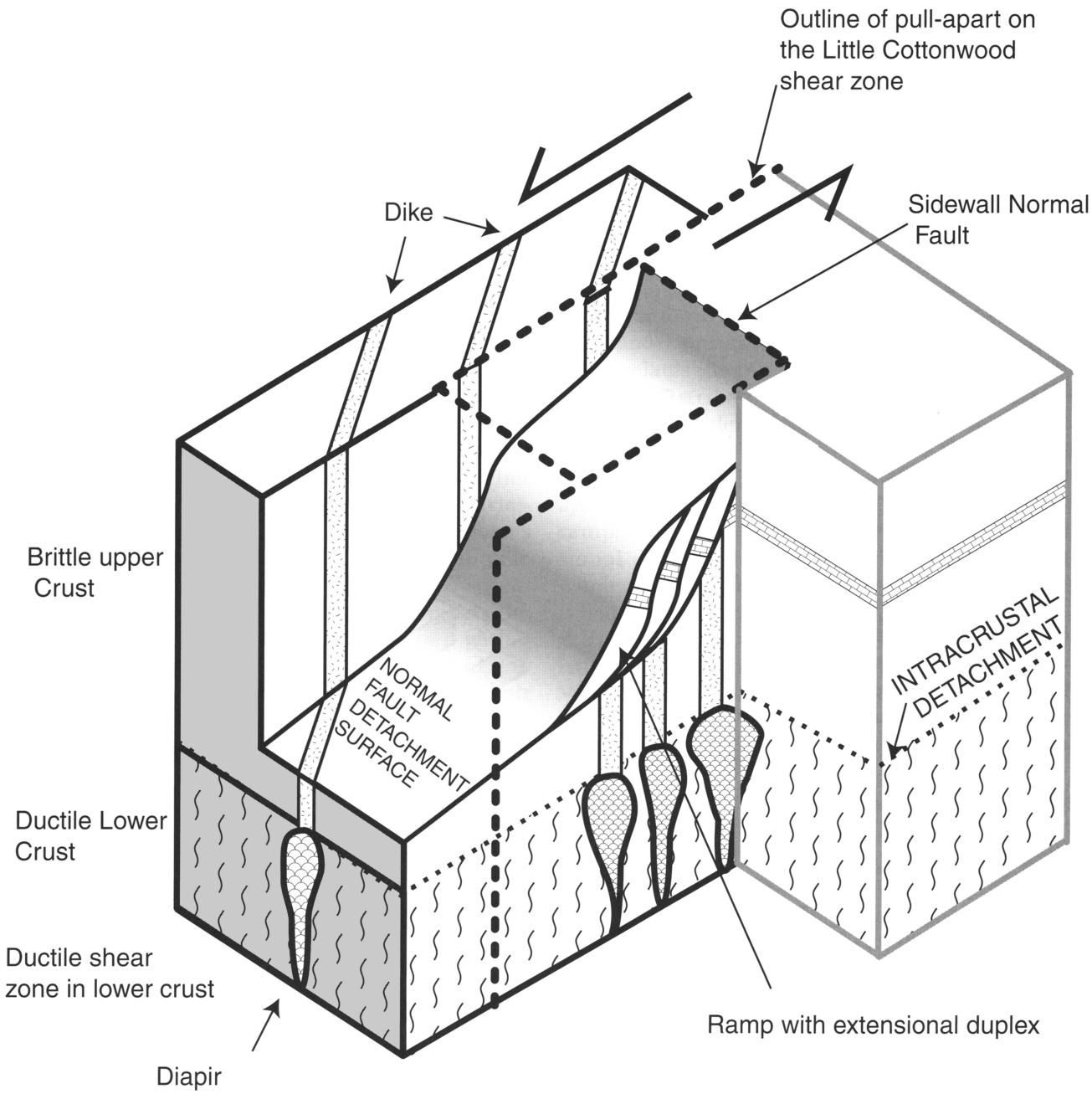

Figure 16. Block diagram illustrating relationship between pull-apart basin, sidewall normal fault, and extensional duplex (at depth).

lead us to propose that the stress field developed as result of localized left-lateral shear deformation on the reactivated suture between Archean and Paleoproterozoic crust. In this context, the dikes would represent T shears (Fig. 14). No finite offset has been measured along the lineament. The east-west trend is in an unfavorable orientation for shear during east-west contraction, so a small displacement is to be expected. It may have been related to changes in slab motion during the waning phases of subduction. A displacement initiated in the lower part of the lithosphere as a broad ductile shear zone will propagate upwards as brittle deformation in the supracrustal rocks (Fig.14). Model experiments demonstrating this situation (Dooley and McClay, 1997; Sims et al. 1999) show that a familiar series of fractures and shears, R, R' (Riedel shears), T (tension fractures), D

(displacement shears), and P (thrust shears) (Skempton, 1966) propagate upward through the cover (Fig. 14). In the experiments these fractures and shears form en-echelon sets that grow in length and become connected by stepover faults that develop into sidewall normal faults bounding pull-apart basins (Fig. 15). In our model, these stepover normal faults develop extensional duplexes at depth, and they provide the initial space for the magma (Fig. 16).

The Little Cottonwood Stock

In map view, the outline of the Little Cottonwood stock is somewhat rectilinear. The northern margin trends east-west and is mostly very steep. At the higher elevations along this margin, the country rock appears to bend over the intrusion as though part of a roof segment (see map in James, 1978). The country rock on the north–south-trending eastern margin is brecciated, and granodiorite contains angular fragments of the country rock. To the east of the intrusion, between it and the Alta stock, the Paleozoic section is repeated three times by linear, roughly north–south-trending normal faults that cross-cut the Sevier thrusts. Some of the stocks cross-cut the dikes, and some of the dikes cross-cut the stocks. Thus, we interpret this extension as being contemporaneous with formation of the dikes and stocks. In this same region, the country rock contains a maze of felsic minor intrusions, all with rectilinear walls (Fig. 18). All these features point to emplacement under brittle conditions. The western margin of the stock is truncated by the Wasatch fault, and the southern margin is complicated by an extensionally reactivated lateral ramp of the Charleston-Nebo thrust.

A sheet of the Mississippian Donut Formation is preserved on top of the stock in the southeast corner. The contact between the Donut Formation and the intrusion is well displayed on the west side of Silver Lake cirque. Just below the contact, the granite contains a thin, 0.5-m-thick layer of mylonite (Fig. 19). It contains sheath folds and a distorted lineation. A detailed chemical study of the mylonite (Szymanski, 1999) indicates that its protolith was granitic rocks of the stock. The mylonite truncates a dike that cuts the granite, and isotopic dates confirm the similarity in age of the granite, shear zone, and dike. The texture of the mylonite shows evidence of dynamic recrystallization. No microscopic kinematic indicators are preserved. On a macroscopic scale the shear zone dips to the west at 43° in a similar direction to the contact of the Donut Formation with the intrusion. Sheath folds in the mylonites are recumbent to gently inclined; axial surface dips range from 9°–42° (mean of 27°) towards 280°. The hinge lines range in plunge from 3°–47° and most are nearly horizontal. The plunge

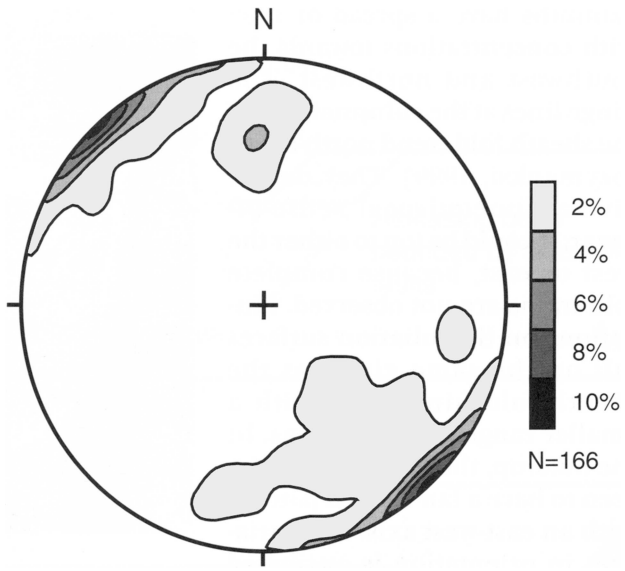

Figure 17. Contoured stereonet of poles to 166 dikes associated with the igneous rocks of the central Wasatch Mountains.

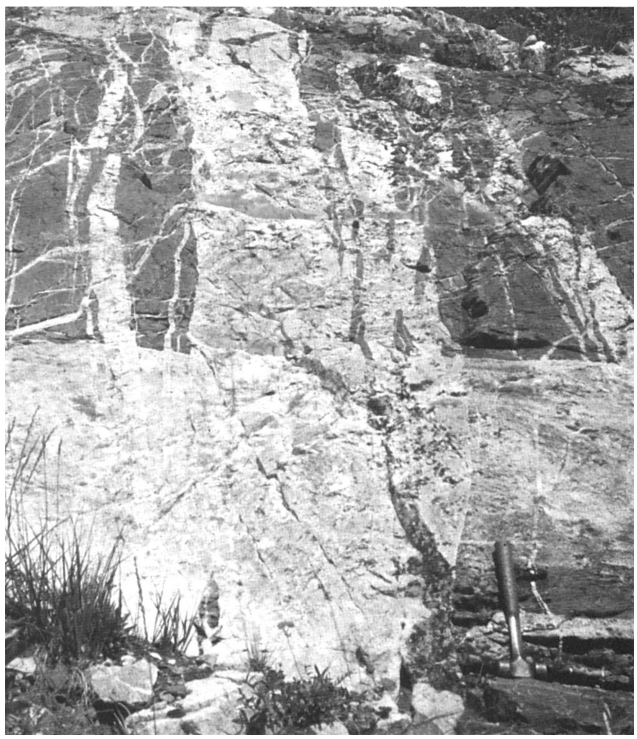

Figure 18. Dike-filled fractures in region between Alta stock and Little Cottonwood stock.

azimuths have a spread of 180° with concentrations towards the southwest and northwest. The hinge lines at the culminations of the sheath fold trend north-south (Szymanksi, 1999). They do not give an unequivocal sense-of-shear; it could be top to either the west or east, because complete fold trains are not observed. Lineations on the foliation surfaces fall on the same girdle as the sheath fold hinges but with a smaller range of orientations. In the outcrop, the lineation can be seen to have a fan-shaped pattern with an east-west axis. The variation in orientation is attributed to a stretching lineation that originated in an east-west direction and was distorted as the mylonite deformed by flattening. In our model, the mylonite formed on the roof fault of an extensional duplex at a depth of about 5.5–6 km. The duplex was associated with a ramp on the listric sidewall fault at the time of intrusion of the stock. The mylonite was later stoped into the magma.

Figure 19. Profile of an isoclinal fold that forms part of a sheath fold in the Silver Lake mylonite zone.

Emplacement Model

Lawton (1980) described the setting of the Little Cottonwood stock and observed that the margins of the pluton did not exhibit a great deal of deformation. He concluded that no more than one third of the space could be accounted for by near-field material transfer processes (Lawton 1980). Our observations of brecciated margins and angular inclusions suggest a brittle rather than a ductile emplacement mechanism, the exception being the Silver Lake mylonite. This is supported by the numerous rectilinear veins of granite in the area between the Little Cottonwood stock and the Alta stock to the east (Fig. 17). We propose that emplacement was assisted by the development of pull-apart structures on the strike-slip zone (Fig. 15) that gave rise to sidewall normal faults with extensional duplexes at depth (Fig. 16). At depth the strike-slip and dip-slip faults merge with the ductile shear zone. In our model, the dikes are interpreted as tension fractures in response to left-lateral slip parallel to the Uinta-Cortez axis. The normal faults between the Little Cottonwood stock and Alta stock represent the remnants of the extensional duplex. The lack of measurable displacement on the proposed shear zone presents a dilemma. The lengths of the pull-apart structures in the Dooley and McClay (1997) models are equal to the displacement on the strike-slip faults. This similarity is not a requirement in natural systems. A relatively long pull-apart basin can develop with small displacement as a result of the spacing of the initial overlapping fractures (Fig. 15) (Dooley and McClay, 1997, front cover of issue). Even a small extension in pull-apart bends creates space that gives rise to subsidence on strike-slip faults. This is a far-field effect, the space being transferred to a convergent zone (i.e., a thrust or subduction zone). However, in cases where a low-density ductile substrate such as salt is involved, intrusion from below may occupy the space created by extension associated with normal faults (Jackson and Vendeville, 1994).

The dikes indicate to us that melts were available and rose along the fractures created by the shear zone. The sharp, linear margins of the Little Cottonwood stock together with the angular inclusions indicate brittle conditions, consistent with fault-controlled emplacement. Two events could have triggered decompression melting of the lower crust: 1) the gravitational collapse of the Sevier orogenic belt (Constenius, 1998) and 2) extension associated with the pull-apart structures along the Little Cottonwood shear zone (new name), a reactivation of the Uinta-Cortez axis. The shear strain on the reactivated Uinta-Cortez axis may have contributed to melting. This would be an

additional control on the linear distribution of the magmas. The magma rose diapirically through the lower crust, following the shear zone. Once it reached the brittle-ductile transition the fractures generated in the brittle crust provided avenues for the dikes we observe. Where there was no impediment the dikes reached the surface and fed the Keetley volcanic field. The magma that formed the Little Cottonwood stock was arrested at a depth of 11–5.5 km (John, 1989a). It ponded in an extensional duplex, which formed on a ramp along the downward extension of the main sidewall fault (Fig. 20). The dikes that followed the tension fractures intersected this highly fractured zone, and the magma was arrested in the space created by extension in the duplex. Magma adjacent to the roof of the duplex became involved in the roof fault shear producing the mylonite. The space created by this mechanism would have been relatively small. The main effect was to arrest the rise of the magma. To produce the additional space we invoke the type of large-scale subsidence proposed for the emplacement of the Ljugaren Granite in Sweden (Cruden, 1998) and the Mount Givens pluton in the Sierra Nevada batholith, California (McNulty et al., 2000) (Fig. 20). The flexural rigidity of the crust below the duplex would have been compromised by the dike swarm, creating the opportunity for large-scale mass transfer of country rock downward into the space created by the rising magma (Fig. 20). The Silver Lake mylonite foundered into the rising magma.

An outcrop in the Albion basin displays a small-scale example of the mechanism just discussed (Fig. 21). Horizontal offset on the margins of the sill can be seen by matching the upper and lower margins and the location of a xenolith (see inset, Fig. 21). The sill terminates in a series of dikes extending below the sill. The space occupied by the dikes fits with the sense of horizontal movement on the sill. We envisage this as an analogue for the extensional duplex. The space occupied by the sill requires that the rocks above were lifted up or the rocks below were dropped. In our model, the rocks below collapsed into the area vacated by the magma.

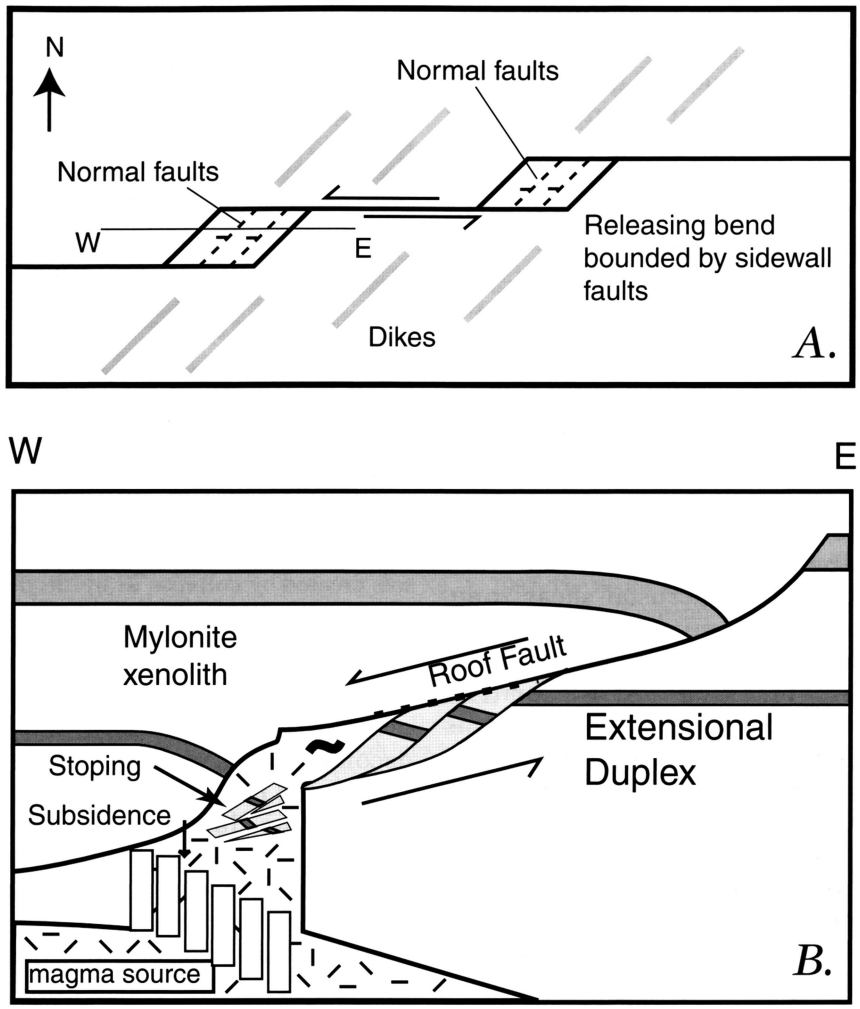

Figure 20. ***A,*** Diagrammatic map of pull-apart. ***B,*** Diagrammatic east-west cross section illustrating large-scale, crustal collapse beneath an extensional duplex (the proposed space-creating mechanism for the Little Cottonwood stock).

The alignment of the stocks with the northern lateral ramp of the Charleston-Nebo thrust may indicate that they were both controlled by the old suture. The right-lateral strike-slip motion required for the northern branch of the collapsing thrust belt is exactly the opposite of that proposed for the emplacement of the magma. We propose that the left-lateral strike-slip motion was related to continued shortening at depth. The right-lateral motion along the lateral ramp was caused by gravitational collapse of the

detached supracrustal thrust stack. This combination of convergence and collapse is similar to the current situation in the Himalayas (Burchfiel et al., 1992)

The other stocks in the central Wasatch Mountains formed in a similar fashion. The development of stepovers, sidewall faults, and extensional duplexes created a continuous weakness along the line now occupied by the stocks. Our model proposes that individual magmas originated from a common source, rose from the ductile shear zone, were guided by low-pressure zones above pull-apart structures in the more brittle supracrustal shear zone, and differentiated on the way up or in the magma chamber after emplacement. At the brittle-ductile transition the magmas were channeled into dikes that either reached the surface, as in the case of the Keetley volcanic field, or were arrested in a manner similar to the sequence of events described for the Little Cottonwood stock. In addition, the lower confining pressure of the higher level stocks may well have allowed them to displace some material upward.

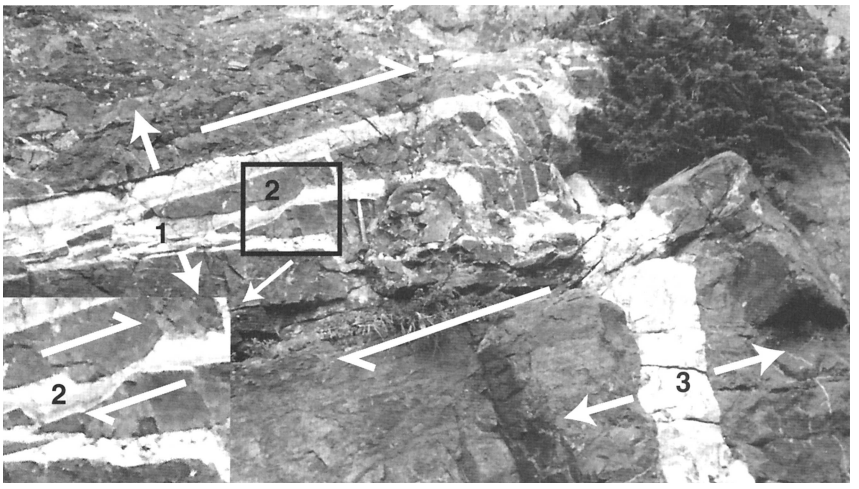

Figure 21. An analogue for the emplacement of the Little Cottonwood stock viewed on an outcrop near the Alta stock. The space occupied by the sills (1) was created by collapse or uplift; our model favors collapse. Slip parallel to the surface occupied by the sill created space for the dikes (3). Note enlarged inset (lower left corner) of area near (2).

CONCLUSIONS

Although the major- and trace element signatures of the igneous rocks from the central Wasatch Mountains resemble typical subduction-related magmas, the high K_2O contents and low ε_{Nd} and ε_{Sr} values are not consistent with magmas generated in a mantle wedge overlying the subducting plate. Our model for these rocks involves partial decompression melting in the mantle associated with gravitational collapse of the orogen followed by intrusion of mafic magma into the lower crust. The input of this extra heat into an already hot, lower crust, in combination with decompression, resulted in widespread and relatively rapid melting of the lower crust and production of a range of magma types. The source rocks for these melts may have been the high-pressure mafic rocks similar in composition to the amphibolites of the Little Willow Formation. Because of the lack of any Eu anomaly, melting either occurred at a depth below plagioclase stability or melt fractions were large (>50% melt) (e.g., either there was no plagioclase or most of the plagioclase was consumed during melting). Ponding of the magma allowed a critical mass to accumulate and differentiate. The volcanic rocks represent a wide variety of small magma bodies that did not pond and coalesce to form a large magma chamber, whereas each stock represents one magma body that ponded and crystallized as a coherent body. Continued melting and extension produced new magmas, but from a similar source, replenishing existing magma bodies. Ascent and emplacement of the igneous rocks of the central Wasatch Mountains are explained as a series of magmas that rose along an east-west trend weakened by the development of an incipient left-lateral strike-slip zone in the brittle upper crust. This zone propagated upward from a ductile shear zone in the lower crust when the suture between Archean and Paleoproterozoic basement was reactivated as a result of continued shortening at depth. Some of the magmas were ponded in extensional duplexes, which developed in association with normal faults that bounded pull-apart basins on the strike-slip zone. The collapse of the crust below the duplexes provided additional space for the parent magmas of the stocks that now form the linear pattern of exposures. Some of these magmas were stored for a long time. They continued to assimilate radiogenic crustal rocks in the highly fractured extensional duplexes and differentiated to relatively evolved magmas, as exemplified by the Little Cottonwood stock. Magma that reached the surface

(Keetley volcanic field) formed without coalescence into larger magma bodies or significant fractionation. The area now occupied by the igneous rocks of the central Wasatch Mountains was overlain by a large volcanic center fed via a planar crustal conduit that developed above a reactivated Paleoproterozoic suture (extension of the Cheyenne belt of southeastern Wyoming).

ACKNOWLEDGMENTS

Many people have contributed to this paper. Paul Layer, Geophysical Institute and Department of Geological Sciences, University of Alaska, Fairbanks, contributed many $^{40}Ar/^{39}Ar$ ages and was very helpful in analysis and discussions of these data. Peter Copeland also provided $^{40}Ar/^{39}Ar$ data. Carmela Garizione, George E. Gehrels, and Damian Hodkinson provided the radiogenic isotopic data. David John made available unpublished chemical and isotopic data, and his insight was invaluable throughout the course of the study. The LA-ICP-MS analyses were done by Lina Patino. INAA analyses were obtained from the Phoenix Laboratory, University of Michigan. Jaeman Lee, Tim Paulson, Ed Wilson, and Dave Szymanski aided in sample collection and fieldwork. Ed Wilson, Cari Corrigan, and Karen Stockstill helped in sample preparation for XRF and LA-ICP-MS analyses. A special thanks goes to Tim Flood who helped with fieldwork and collected some of the $^{40}Ar/^{39}Ar$ data and to Tim Holst who introduced us to the area and helped with data collection. David John, Eric Christiansen, and Ricardo Presnell provided careful reviews that substantially improved the paper.

REFERENCES CITED

Atkin, S. A., 1982, Magmatic history, alteration and mineralization of the Clayton Peak stock, Utah [Ph.D. dissert.]: Baltimore, Maryland, The Johns Hopkins University, 395 p.

Barr, D. B., 1993, Time, space, and composition patterns of middle Cenozoic mafic to intermediate compositions lava flows of the Great Basin, western U. S. A. [M.S. thesis]: Provo, Utah, Brigham Young University, 68 p.

Best, M. B., and Christiansen, E. H, 1991, Limited extension during peak Tertiary volcanism, Great Basin of Nevada and Utah: Journal of Geophysical Research, v. 96, p. 13, 509–13,528.

Bromfield, M. D., Erickson, A J., Jr., Haddadin, M. A., and Mehnert, H. H., 1977, Potassium-argon ages of intrusion, extrusion and associated ore deposits, Park City mining district, Utah: Economic Geology, v. 72, p. 837–848.

Bryan, W. B., Finger, L. W., and Chayes, R., 1969, Estimating proportion in petrographic mixing equations by least squares approximation: Science, v. 163, p. 926–927.

Bryant, B., 1988, Evolution, and Early Proterozoic history of the margin of the Archean continent in Utah, *in* Ernst, W. G., ed., Metamorphism and crustal evolution of the western United States: Englewood Cliffs, New Jersey, Prentice Hall, p. 431–445.

___ 1990, Geologic map of the Salt Lake City 30'x60' quadrangle, north-central Utah, and Uinta County, Wyoming: U. S. Geological Survey Miscellaneous Investigations Series Map 1-1944, scale 1:100,000, 2 sheets.

___ 1992, Geologic and structure maps of the Salt Lake City 1° x 2° Quadrangle, Utah and Wyoming: U. S. Geological Survey Miscellaneous Investigation Series Map I-1997, scale 1:125,000, 3 sheets.

Bryant, B., and Nichols, D. J., 1988, Late Mesozoic and early Tertiary reactivation of an ancient crustal boundary along the Uinta trend and its interaction with the Sevier orogenic belt, *in* Schmidt, C. J. and Perry, W. J., Jr., eds., Interaction of the Rocky Mountain foreland and the Cordilleran thrust belt: Boulder, Colorado, Geological Society of America Memoir 171, p. 411–430.

Burchfiel, B. C., Chen, Z., Hodges, K. V., Liu, Y., Royden, L. H., Deng, C., and Xu, J., 1992, The South Tibetan detachment fault system, Himalayan orogen: Contemporaneous with and parallel to shortening in a collisional mountain belt: Geological Society of America Special Paper 269, 41 p.

Cambray, F. W., and Holst, T. B., 1993, Kinematics of emplacement of the Tertiary Alta pluton, central Wasatch Mountains, Utah [abs.]: Eos, American Geophysical Union, v. 74, no. 43, supplement, p. 578.

Coney, P. J., and Reynolds, S. J., 1977, Cordilleran Benioff zones: Nature, v. 270, p. 403–406.

Constenius, K. N., 1996, Late Paleogene extensional collapse of the Cordilleran foreland fold and thrust belt: Geological Society of America Bulletin, v. 108, p. 20–39.

___ 1998, Extensional tectonics of the Cordilleran fold-thrust belt and the Jurassic-Cretaceous Great Valley forearc basin, [Ph.D. dissert.]: Tucson, University of Arizona, 116 p.

___ 1999, Structural evolution of the Uinta salient and tectonomagmatic rejuvenation of the Cheyenne belt, north-central Utah [abs.]: American Association of Petroleum Geologists Bulletin, v. 83, p. 1181.

Constenius, K. N., Gehrels, G. E., Flood, T .P., Layer, P. W., and Copeland, P., 1997, Deer Creek detachment fault system, Wasatch Mountains, Utah: Geological Society of America Abstracts with Programs, v. 29, no. 6, A380.

Criss J. W., 1980, Fundamental parameter calculation on a laboratory microcomputer: Advances in X-ray Analysis, v. 23, p. 93–97.

Crittenden, M. D., Jr., Stuckless, J. S., Kistler, R. W., and Stern, T. W., 1973, Radiometric dating of intrusive rocks in the Cottonwood area, Utah: U.S. Geological Survey Journal of Research, v. 1, p. 173–178.

Cross, T. A., and Pilger, R. H., Jr., 1978, Constraints on absolute motion and plate interaction inferred from Cenozoic igneous activity in the western United States: American Journal of Science, v. 278, p. 865–902.

Cruden, A. R., 1998, On the emplacement of tabular granites: Journal of the Geological Society (London), v. 155, p. 853–862.

Demars, L. C., 1956, Geology of the northern part of Dry Mountain, southern Wasatch Mountains, Utah: Provo, Utah, Brigham Young University Geology Studies, v. 3, no. 2, 49 p.

DePaolo, D. J. and Wasserburg, G. J., 1976, Nd isotopic variations and petrogenetic models: Geophysical Research Letters, v. 3, p. 249–252.

Dickinson, W. R., 1991, Tectonic setting of faulted Tertiary strata associated with the Catalina core complex in southern Arizona: Geological Society of America Special Paper 264, 106 p.

Dooley, T., and McClay, K., 1997, Analog modeling of pull-apart basins: American Association of Petroleum Geologists Bulletin, v. 81, p. 1804–1826.

Eardley, A. J., 1933, Stratigraphy of the southern Wasatch Mountains, Utah: Michigan Academy of Science Papers, v. 18, p. 307–344.

Engebretson, D. C., Cox, A., and Gordon, R. G., 1985, Relative motions between oceanic and continental plates in the Pacific basin: Geological Society of America Special Paper 206, 59 p.

England, P. C., and Houseman, G. A., 1988, The mechanics of the Tibetan Plateau: Philosophical Transactions of the Royal Society of London, series A, v. 326, p. 301–329.

Farmer, G. L., and DePaolo, D. J., 1983, Origin of Mesozoic and Tertiary granite in the western United States and implications for pre-Mesozoic crustal structure: 1. Nd and Sr isotopic studies in the geocline of the northern Great Basin: Journal of Geophysical Research, v. 88, p. 3379–3401.

___ 1984, Origin of Mesozoic and Tertiary granite in the western United States and implications for pre-Mesozoic crustal structure: 2. Nd and Sr isotopic studies of unmineralized and Cu- and Mo-mineralized granite in the Precambrian craton: Journal of Geophysical Research, v. 89, p. 10,141–10,160.

Feher, L., 1997, Petrogenesis of the Keetley Volcanics in Summit and Wasatch Counties, north-central Utah [M.S. thesis]: East Lansing, Michigan State University, 95 p.

Gibbs, A. D., 1984, Structural evolution of extensional basin margins: Journal of the Geological Society (London), v. 141, p. 609–620.

Gill, J. B., 1981. Orogenic sndesites and plate tectonics: Berlin, Springer, 389 p.

Hannah, R. S., Vogel, T. A., Patino, L. C., Alvarado, G. E., Perez, W. and Smith, D. R., 2001, Origin of the silicic volcanic rocks in central Costa Rica: A study of a chemically variable ash-flow sheet in the Tiribí Tuff: Bulletin of Volcanology, in press.

Hanson, S. L., 1995, Mineralogy, petrology, geochemistry and crystal size distribution of Tertiary plutons of the central Wasatch Mountains, Utah [Ph.D. dissert.]: Salt Lake City, University of Utah, 371 p.

Hedge, C. E., Stacey, J. S., and Bryant, B., 1983, Geochronology of the Farmington Canyon complex, Wasatch Mountains, Utah, *in* Miller, D. M., Todd, V. R. and Howard, K. A., eds., Tectonic and stratigraphic studies in the eastern Great Basin: Boulder, Colorado, Geological Society of America Memoir 157, p. 33–44.

Hintze, L. F., 1988, Geological history of Utah: Provo, Utah, Brigham Young University Geological Studies Special Publication 7, 202 p.

Hodges, K. V., 1991, Pressure-temperature-time paths, Annual Reviews of Earth and Planetary Sciences: v. 19, p. 207–236.

Hutton, D.H.W., 1988, Granite emplacement mechanisms and tectonic controls: inferences from deformation studies: Transactions of the Royal Society of Edinburgh: Earth Sciences, v. 79, p. 245–255.

Jackson, M.P.A., and Vendeville, B. C., 1994, Regional extension as a geologic trigger for diapirism: Geological Society of America Bulletin, v. 106, p. 57–73.

James, P. L., 1978, Geology, ore deposits and history of the Big Cottonwood mining district, Salt Lake County, Utah: Utah Geological and Mineralogical Survey Bulletin 114, 98 p.

John, D. A., 1989a, Geologic setting, depths of emplacement, and regional distribution of fluid inclusions in intrusions of the central Wasatch Mountains, Utah: Economic Geology, v.84, p. 386–409.

___ 1989b, Evolution of hydrothermal fluids in the Park Premier stock, central Wasatch Mountains, Utah: Economic Geology, v. 84, p. 879–902.

___ 1992, Evolution of the hydrothermal fluids in the Alta stock, Utah: U.S. Geological Survey Bulletin 1977, 51 p.

John, D. A., Turrin, B. D., and Miller, R. J., 1998, New K-Ar and $^{40}Ar/^{39}Ar$ ages of plutonism, hydrothermal alteration, and mineralization in the central Wasatch Mountains, Utah, *in* John, D. A. and Ballantyne, G. H., eds., Geology and ore deposits of the Oquirrh and Wasatch Mountains, Utah: Guidebook Series, v. 29, Society of Economic Geologists, p. 47–57.

Kohlmann, N.A.J., 1980, The polymetamorphism of the Little Willow Formation, Wasatch Mountains, Utah [M.S. thesis]: Duluth, University of Minnesota, 119 p.

Lawton, T. F., 1980, Petrography and structure of the Little Cottonwood stock and metamorphic aureole, central Wasatch Mountains, Utah [M.S. thesis]: Palo Alto, California, Stanford University, 76 p.

LeBas, M. J., Le Maitre, R. W., Streckeisen, A., and Zanettin, B., 1986, A chemical classification of volcanic rocks based on the total alkali-silica diagram: Journal of Petrology, v. 27, p. 745–750.

Leveinen, J. E., 1994, Petrology of the Keetley Volcanics in Summit and Wasatch Counties, north-central Utah [M.S. thesis]: Duluth, University of Minnesota, 175 p.

Lipman, P. W., 1980, Cenozoic volcanism in the western United States: Implications for continental tectonics, *in* Studies in geophysics—continental tectonics: Washington, D. C., National Academy of Sciences, p. 161–174.

Lipman, P. W., 1992, Magmatism in the Cordilleran United States: Progress and problems, *in* Burchfiel, B. C., Lipman, P. W., and Zoback, M. L. eds., The Cordilleran orogen: Conterminous U. S.: Boulder, Colorado, Geological Society of America, Geology of North America, v. G-3, p. 481–514

Lister, G. S., and Baldwin, S. L., 1993, Plutonism and the origin of metamorphic core complexes: Geology, v. 21, p. 607–610.

Marsh, A. J., 1992, Petrology of the northeast portion of the Little Cottonwood stock and associated contact metamorphic aureole, central Wasatch Mountains, Utah [M.S. thesis]: San Antonio, University of Texas at San Antonio, 167 p.

Marsh, A. J., and Smith, R. K., 1997, The Oligocene Little Cottonwood stock, central Wasatch Mountains, Utah: An example of compositional zoning by side-wall fractional crystallization of an arc-related intrusion: The Mountain Geologist, v. 34, p. 83–95.

McNulty, B. A., Tobisch, O. T., Cruden, A. R., and Gilder, S., 2000, Multistage emplacement of the Mount Givens pluton, central Sierra Nevada batholith, California: Geological Society of America Bulletin, v. 112, p. 119–135.

Mills, J. G., Jr, Saltoun, B. J., and Vogel, T. A., 1997, Magma batches in the Timber Mountain magmatic system, southwestern

Nevada volcanic Field, Nevada, USA: Journal of Volcanology and Geothermal Research, v. 178, p. 185–208.

Morris, G. A., Larson, P. B., and Hooper, P. R., 2000, 'Subduction style' magmatism in a non-subduction setting: the Colville igneous complex, NE Washington State, USA: Journal of Petrology, v. 41, p. 43–67.

Naeser, C. W., Bryant, B., Crittenden, M. D., Jr., and Sorensen, M. L., 1983, Fission-track ages of apatite in the Wasatch Mountains, Utah: An uplift study, *in* Miller, D. M., Todd, V. R., and Howard, K. A., eds., Tectonic and stratigraphic studies in the eastern Great Basin: Boulder, Colorado, Geological Society of America Memoir 157, p. 29–36.

Palmer, J. O., 1974, Petrology of the Clayton Peak stock, a zoned pluton near Brighton, Utah: Provo, Utah, Brigham Young University Geologic Studies, v. 21, p. 177–214.

Parry, W. T., and Bruhn, R. L., 1987, Fluid inclusion evidence for minimum 11 km vertical offset on the Wasatch fault, Utah: Geology, v. 15, p. 67–70.

Paterson, S. R., and Fowler, T.K.J., 1993, Re-examining pluton emplacement processes: Journal of Structural Geology, v. 15, p. 191–206.

Paterson, S. R., and Schmidt, K. L., 1999, Is there a close spatial relationship between faults and plutons?: Journal of Structural Geology, v. 21, p. 1131–1142.

Patino, L. C., 1997, Geochemical characterization of Central American subduction zone system: Slab input, output from volcanoes, and slab-mantle interactions [Ph.D. dissert.]: New Brunswick, New Jersey, Rutgers University, 183 p.

Paulsen, T., and Marshak, S., 1998, Charleston transverse zone, Wasatch Mountains, Utah: Structure of the Provo salient's northern margin, Sevier fold-thrust belt: Geological Society of America Bulletin, v. 110, p. 512–522.

Presnell, R. D., 1992, Local and regional geology of the Oquirrh Mountains, *in* Wilson, J. R., ed., Field guide to geologic excursions in Utah and adjacent areas of Nevada, Idaho, and Wyoming: Utah Geological Survey Miscellaneous Publication 92-3, p. 293–306.

___ 1998, Structural controls on the plutonism and metallogeny in the Wasatch and Oquirrh Mountains, Utah, *in* John, D. A. and Ballantyne, G. H., eds., Geology and ore deposits of the Oquirrh and Wasatch Mountains: Guidebook Series, v. 29, Society of Economic Geologists, p. 1–10.

Roberts, M. P., and Clemens, J. D., 1993, Origin of high-potassium, calc-alkaline, I-type granitoids: Geology, v. 21, p. 825–828.

Roberts, R. J., Crittenden, M. D., Jr., Tooker, E. W., Morris, H. T., Hose, R. K., and Cheney, T. M., 1965, Pennsylvanian and Permian basins in northwestern Utah, northeastern Nevada and south-central Idaho: American Association of Petroleum Geologists Bulletin, v. 49, p. 1926–1956.

Rowley, P. D., 1998, Cenozoic transverse zones and igneous belts in the Great Basin, western United States: Their tectonic and economic implications, *in* Faulds, J. E., and Stewart, J. H., eds., Accommodation zones and transfer zones: the regional segmentation of the Basin and Range province: Geological Society of America Special Paper 323, p. 195–228.

Scales, J. R., 1972, Geology and petrography of igneous rocks in the Park mountain area, Park City, Utah [M. S. thesis]: Iowa City, University of Iowa, 108 p.

Sims, D., Ferrill, D. A., and Stamatakos, J. A., 1999, Role of a ductile decollement in the development of pull-apart basins: Experimental results and natural examples: Journal of Structural Geology, v. 21, p. 533–554.

Skempton, A. W., 1966, Some observations on tectonic shear zones: Proceedings of the 1st Congress of the International Society of Rock Mechanics, Lisbon, Portugal, v. 1, p. 329–335.

Springer, W., and Seck, H. A., 1997, Partial fusion of basic granulites at 5 and 15 kbar: implications for the origin of TTG magmas: Contributions to Mineralogy and Petrology, v. 127, p. 30–45.

Sterne, E. J., and Constenius, K. N., 1997, Space-time relationships between magmatism and tectonism in the western United States between 120 Ma and 10 Ma: a regional context for the Front Range of Colorado, *in* Bolyard, D. W., and Sonnenberg, S. A., eds., Geologic history of the Colorado Front Range: Denver, Colorado, The Rocky Mountain Association of Geologists, 1997 RMS-AAPG Field Trip #7, p. 85–100.

Stone, D. S., 1993, Tectonic evolution of the Uinta µountains: Palinspastic restoration of a structural cross section along longitude 109° 15', Utah: Utah Geological Survey Miscellaneous Publication 93-8, 19 p.

Streckeisen, A., 1976, To each plutonic rock its proper name: Earth Science Reviews, v. 12, p. 1–33.

Sun, S. S., and McDonough, W. F., 1989. Chemical and isotopic systematics of oceanic basalts: implications for mantle compositions and processes, *in* Saunders, A. D., and Norry, M. J., eds., Magmatism in the ocean basins: Geological Society Special Publication no. 42, p. 313–345.

Szymanski, 1999, Faulting in an extensional environment: an emplacement mechanism for the Little Cottonwood stock, central Wasatch Mountains, Utah: [M.S. thesis]: East Lansing, Michigan State University, 93 p.

Vogel, T. A., Cambray, F. W., Feher, L., Constenius, K. N., and the WIB Research Team, 1998, Petrochemistry and emplacement history of the Wasatch igneous belt, *in* John, D. A., and Ballantyne, G. H., eds., Geology and ore deposits of the Oquirrh and Wasatch Mountains, Utah: Guidebook Series, v. 29, Society of Economic Geologists, p. 35–46.

Waite, K. A., and six others,1998, Petrogenesis of the volcanic and intrusive rocks associated with the Bingham Canyon porphyry Cu-Au-Mo deposit, Utah, *in* John, D. A., and Ballantyne, G. H., eds., Geology and ore deposits of the Oquirrh and Wasatch Mountains, Utah: Guidebook Series, v. 29, Society of Economic Geologists, p. 69–90.

Ward, P. L., 1995, Subduction cycles under western North America during the Mesozoic and Cenozoic eras, *in* Miller, D. M., and Busby, C., eds., Jurassic magmatism and tectonics of the North American Cordillera: Geological Society of America Special Paper 299, p. 1–45.

Wernicke, B., 1992, Cenozoic extensional tectonics of the U.S. Cordillera, *in* Burchfiel, B. C., Lipman, P. W., and Zoback, M. L., eds., The Cordilleran orogen: Conterminous U.S.: Boulder, Colorado, Geological Society of America, The Geology of North America, v. G-3, p. 553–582

Wilson, J. C., 1961, Geology of the Alta stock [Ph.D. dissert.]: Pasadena, California Institute of Technology, 236 p.

Woodfill, R. D., 1972. A geologic and petrographic investigation of a northern part of the Keetley volcanic field, Summit and Wasatch Counties, Utah [Ph.D. dissert.]: West Lafayette, Indiana, Purdue University, 168 p.

Wright, J. E., and Snoke, A. W., 1993, Tertiary magmatism and mylonitization in the Ruby-East Humboldt metamorphic core complex, northeastern Nevada: U-Pb geochronology and Sr, Nd, and Pb isotope geochemistry: Geological Society of America Bulletin, v. 105, p. 935–952.

Wright, T. L., and Doherty, P. C., 1970, A linear programming and least squares computer method for solving petrologic mixing problems: Geological Society of America Bulletin, v. 81, p. 1995–2008.

MANUSCRIPT SUBMITTED DECEMBER 1, 2000
REVISED MANUSCRIPT RECEIVED NOVEMBER 15, 2001
MANUSCRIPT ACCEPTED NOVEMBER 26, 2001